INFLUENCE OF SOURCE STRENGTH ON THE CRITICAL BEHAVIOR OF URANYL NITRATE SOLUTIONS

by

Gerald Bruce Dulco

A Thesis Submitted to the Faculty of the

DEPARTMENT OF NUCLEAR ENGINEERING

In Partial Fulfillment of the Requirements
For the Degree of

MASTER OF SCIENCE

In the Graduate College

THE UNIVERSITY OF ARIZONA

1 9 8 2

STATEMENT BY AUTHOR

This thesis has been submitted in partial fulfillment of requirements for an advanced degree at The University of Arizona and is deposited in the University Library to be made available to borrowers under rules of the Library.

Brief quotations from this thesis are allowable without special permission, provided that accurate acknowledgment of source is made. Requests for permission for extended quotation from or reproduction of this manuscript in whole or in part may be granted by the head of the major department or the Dean of the Graduate College when in his judgment the proposed use of the material is in the interests of scholarship. In all other instances, however, permission must be obtained from the author.

SIGNED: Gerald B. Dulco

APPROVAL BY THESIS DIRECTOR

This thesis has been approved on the date shown below:

Robert L. Seale — 5 May 1982

ROBERT L. SEALE — Date

Professor of Nuclear Engineering

To My Father, Mother and Jacque

ACKNOWLEDGMENTS

The author would like to thank Dr. Robert Seale for his assistance and direction in the preparation of this thesis.

I have been aided through phone conversations by many persons in the preparation of this thesis and wish to thank H. M. Forehand, G. E. Hansen, U. Jenquin, R. C. Lloyd, and W. Waltz for their help. In particular, I wish to thank Dr. David Johnson whose several phone conversations and use of his publication provided an accurate method in determining the results of Chapters 3 and 4.

A special debt of gratitude is expressed to Dr. Robert Miles whose valuable assistance with the computer program "ANSOURCE" made it possible to use Johnson's method.

Finally, deep appreciation is expressed to my wife, Jacque, for her patience in the preparation of this thesis and who truly provided the greatest inspiration of all.

TABLE OF CONTENTS

		Page
	LIST OF ILLUSTRATIONS	vi
	LIST OF TABLES	vii
	ABSTRACT	viii
1.	INTRODUCTION	1
2.	THEORY	9
	2.1 The Probability, W, of a Source Neutron Sponsoring a Persistent Fission Chain	10
	2.2 The Definition of a Strong and Weak Neutron Source	12
	2.3 The Probability Distribution in Time of the Occurrence of a Fission Burst Following a Ramp Increase of Reactivity	14
	2.4 Summary	21
3.	ACTUAL EXPERIENCE WITH CRITICAL SOLUTIONS	24
	3.1 The CRAC Experiments	25
	3.2 Nuclear Incident at the ICPP on January 25, 1961	42
	3.3 Accidental Criticality at Wood River Junction, R.I. on July 24, 1964	53
4.	THE AGNS DISSOLVER TANK	60
5.	CONCLUSIONS AND SUMMARY	72
	APPENDIX A: REACTIVITY ANALYSIS	76
	APPENDIX B: COMPUTER PROGRAMS	80
	REFERENCES	100

LIST OF ILLUSTRATIONS

Figure		Page
2.1.	Power and reactivity vs time	15
3.1.	Infinite multiplication factor vs uranium concentration	30
3.2.	Geometric buckling vs U-235 concentration . . .	31
3.3.	U-235 concentration vs neutron lifetime	33
3.4.	Reactivity vs height of 300 mm dia cylinder . .	36
3.5.	Reactivity vs height of 800 mm dia cylinder . .	37
3.6.	Probability of the first persistent fission chain under a ramp insertion	39
3.7.	Integration of probability vs distribution of experiments	41
3.8.	Number of CRAC experiments per interval vs distribution of experiments	43
3.9.	Process flowsheet for H-cell first cycle product wash	44
3.10.	Specific power at peak of first pulse vs reciprocal period for the 800 mm dia cylinder . .	51
3.11.	Specific power at peak of first pulse vs reciprocal period for the 300 mm dia cylinder . .	57
3.12.	Integration of probability vs $(aS_{eff}/\overline{\nu}\Gamma_2)^{\frac{1}{2}}t$ . .	59
4.1.	Probability of the first persistent fission chain under a ramp insertion	69

LIST OF TABLES

Table		Page
1.1.	Criticality incidents involving solution systems	2
3.1.	Spontaneous fission source strengths for twenty-nine CRAC experiments	27
3.2.	Data for Figure 3.1	29
3.3.	Data for Figure 3.3	32
3.4.	Source condition for twenty-nine CRAC experiments	35
3.5.	Distribution of fission bursts	40
3.6.	Reactivity addition rate for the ICPP	53
3.7.	Reactivity addition rates for WRJ	58
4.1.	Isotopic composition of Yankee Rowe Reactor fuel	63
4.2.	Fuel assembly fissile material inventory	65
4.3.	Spontaneous neutron emission rates for uranium and plutonium isotopes	66

ABSTRACT

A one-group calculation comparing the critical behavior of uranyl nitrate solutions for low and high enrichments has been made. This involved experiments 93% enriched in U-235, and a dissolver tank having a maximum enrichment of 5%.

In the experiments using highly enriched uranium, solutions having a wide range of concentration were injected into cylinders beyond the volume sufficient for criticality. For 29 separate experiments fission bursts were observed to occur at different times with yields that were not predictable using standard kinetics. This study examined these experiments on the basis of a technique developed by Hansen. Two criticality accidents were then considered and the results concurred with the findings of the KEWB experiments.

The AGNS dissolver tank, designed to accommodate the initial step in fuel reprocessing, was then considered and it was found that the probability of a large burst accident is vanishingly small.

CHAPTER 1

INTRODUCTION

Since the beginning of the nuclear industry, there have been twelve incidents where an accidental criticality occurred in a solution system. Due to unplanned and unexpected changes in these systems, the reactivity exceeded the critical condition. High gamma and neutron radiation levels resulted. In order to familiarize the reader with these events, Table 1.1 is provided such that the causes of these criticality incidents may be briefly summarized. This information was put together using data from McLaughlin (1978), Paxton (1972) and Stratton (1967). It is worthwhile to note that these "operational abnormalities" are becoming more and more infrequent.

A system is said to be critical if a neutron population, once established, will maintain itself constant, i.e., neither increasing nor decreasing in time. All factors that influence the interaction of neutrons with matter affect the circumstances under which criticality is achieved.

If a self-sustaining fissioning system is altered such that the neutron population increases with time, the system is said to be supercritical. If, on the other hand, a self-sustaining fissioning system is altered such that the

Table 1.1. Criticality incidents involving solution systems.

DATE	LOCATION	ACTIVE MATERIAL	GEOMETRY	TOTAL FISSIONS	CAUSE	PERSONNEL EXPOSURE
December 1949	LASL New Mexico	~1kgm U-235 $UO_2(NO_3)_2$ in 13.6 liters of water	Spherical Graphite reflected	$3\text{-}4 \times 10^{16}$	(Water Boiler Reactor) Poison control rods removed manually	Operator received 2.5 rem of gamma radiation
November 16, 1951	Hanford Works Richland, WA	1.15 kgm Pu $PuO_2(NO_3)_2$ in 63.8 liters of water	Spherical (93% full) unreflected	8×10^{16}	Cadmium rod removed too rapidly, remote control	None $PuO_2(NO_3)_2$ solution contaminated experimental area
May 26, 1954	ORNL Tennessee	18.3 kgm U-235 UO_2F_2 in 55.4 liters of water	Cylindrical Annulus unreflected	1×10^{17}	Central poison cylinder tilted to a less favorable position	Because of thick shielding, no person received greater than 0.9 rem
February 1, 1956	ORNL Tennessee	27.7 kgm U-235 UO_2F_2 in 58.9 liters of water	Cylindrical unreflected	1.6×10^{17}	Wave motion created by falling cd sheet created a critical geometry	No person was irradiated in an amount greater than 0.6 rem
June 16, 1958	Y-12 Processing Plant Oak Ridge, TN	2.5 kgm U-235 $UO_2(NO_3)_2$ in 56.1 liters of water	Cylindrical Bottom was concrete reflected	1.3×10^{18}	Uranium Process Solution added to wash water in 55 gallon drum	8 people irradiated in the amounts of 461, 428, 413, 431, 298, 36.5, and 28.8 rem
December 30, 1958	LASL Pu Processing Plant New Mexico	3.27 kgm Pu $PuO_2(NO_3)_2$ in 168 liters of water	Cylindrical Bottom was water reflected	1.5×10^{17}	Agitator in Pu process tank created a critical geometry	Operator died 36 hrs later and two people received doses of 134 and 53 rem

Table 1.1.--Continued

DATE	LOCATION	ACTIVE MATERIAL	GEOMETRY	TOTAL FISSIONS	CAUSE	PERSONNEL EXPOSURE
October 16, 1959	Idaho Chemical Processing Plant IRTA, Idaho	34.5 kgm U-235 $UO_2(NO_3)_2$ in 800 liters of water	Cylindrical Bottom was concrete reflected	4×10^{19}	Uranium Process Solution siphoned from safe to unsafe geometry	Beta dosages were 50 and 52 rem for 2 people, & 17 persons also received small amounts
January 25, 1961	Idaho Chemical Processing Plant IRTA, Idaho	8 kgm U-235 $UO_2(NO_3)_2$ in 40 liters of water	Cylindrical unreflected	6×10^{17}	Uranium Process Solution pumped from safe to unsafe geometry	Irradiations were trivial since process cell provided extensive shielding
April 7, 1962	Hanford Works Richland, WA	1.55 kgm Pu 46 liters of Pu solution	Cylindrical unreflected	8.2×10^{17}	Pu solution incorrectly siphoned to floor of a solvent extraction hood	3 people received exposures of 110, 45, & 19 rem
July 24, 1964	United Nuclear Corp. Wood River Jct., R.I.	2.64 kgm U-235 41 liters of $UO_2(NO_3)_2$ soln	Cylindrical unreflected	1.3×10^{17}	Operator poured 93% enriched $UO_2(NO_3)_2$ solution into a Na_2CO_3 makeup tank thinking it was TCE	Operator received an exposure of 10,000 rads & died 49 hrs later. 2 others received 60-100 rads
August 24, 1970	Windscale Works England	~2 kgm Pu 50 liters of $PuO_2(NO_3)_2$ soln	Cylindrical "hole" in solvent layer	1×10^{15}	Pu solution flowed into a vessel creating an emulsion layer of decrease reactivity	2 people received exposures: one less than 1 rad, the other less than 2 rads
October 17, 1978	Idaho Chemical Processing Plant IRTA, Idaho	An unknown amount of uranium in a $Al(NO_3)_3$ scrub solution	Cylindrical unreflected	$\sim 3 \times 10^{18}$	$Al(NO_3)_3$ scrub sol'n was .08M instead of .75M; sol'n acted as a stripper resulting in an increase in uranium concentration	17 people received whole-body exposure with a maximum whole-body dose of less than 130 rem

neutron population decreases with time, the system is said to have become subcritical. Specifically k, a quantitative measure of the state of such systems, is the ratio of the neutron population at time $(t + \ell)$ to the neutron population at time t, where ℓ is the neutron generation time. If $k = 1$, the system is critical. For systems where $k > 1$, the system is supercritical; for $k < 1$, the system is subcritical. The severity of a criticality accident is, in part, determined by how much excess reactivity, δk_{max}, is inserted into the system before some overriding quenching mechanism intervenes to reduce the multiplication, k, below unity.

Nuclear criticality safety is defined by the American National Standards Institute as "the prevention or termination of inadvertent nuclear chain reactions in nonreactor environments." The primary emphasis is on prevention and the usually accepted level of appropriate prevention is guided by the double-contingency principle. This rule calls for controls such that no single mishap or malfunction can lead to a criticality accident regardless of its probability of occurrence. Therefore, at least two independent events, not necessarily concurrent, must occur before a condition of criticality would be possible.

In the usual consideration of the response of a nuclear system to a change in multiplication, the basic problem to be solved is the evaluation of the change in a fixed, predictable neutron population from a level n_1 to a

level n_2 as a consequence of the change in multiplication. The initial population is assumed to be well defined and finite, and the response of the system to a change in multiplication is governed by the "standard kinetics" equation for such systems. Generally, such systems are initially critical and have a spatial neutron population which is represented by the solution to the transport or diffusion equation for such systems.

There arises a problem, however, when a system is initially subcritical and is without an already existing neutron population. As an example, consider a solution of liquid uranium salt contained in a geometry such that its multiplication is well below critical. No fissions are possible unless a "chance" neutron happens to trigger a decaying chain of fissions. This chain may generate a few neutrons, but since $k << 1$, it will quickly vanish. If this solution were to be pumped into a critical geometry, or even to a super-critical geometry, the response of the neutron population in the solution would depend both on the value of k as a function of time, and on the time at which the neutron needed to initiate fission chains is first available to the solution. It is possible that solution in a geometry that is well beyond the critical condition would not have fissions occurring if there are no neutrons present to trigger the first fission reaction in the chain. Under these conditions,

it is quite possible that a large supercritical condition could be achieved prior to the availability of a first neutron and hence a rather impressive "burst" could result.

In this study, our objective is a detailed examination of the behavior of critical systems in the presence of sources of differing strengths. In particular, given a ramp increase of reactivity in a multiplying solution, it is of interest to determine what conditions of neutron source strength lead to a "standard kinetics" response, and under what circumstances, the criterion for a "delayed burst" is met. In Chapter 3, our attention will focus on systems of high enrichment, whereas Chapter 4 will deal with a system of low enrichment.

Since a thorough understanding of the parameters of importance in criticality accidents is essential, the Service d' Études de Criticité of the French Commissariat à l' Énergie Atomique initiated a program designated "Consequences Radiologiques d' un Accident de Criticité" (CRAC) in November 1968. Experiments were performed in which aqueous uranyl nitrate solutions at various concentrations were injected into 300 mm and 800 mm diameter pipes to heights in excess of the critical height. The uranium was 93% enriched and the results gave valuable insight into the behavior to be expected with accidental supercritical accumulations of fissile material.

The results of the CRAC experiments have been evaluated for the effects of source strength using a general analysis developed by Dr. G. E. Hansen (1960), for the behavior of critical systems assembled in the presence of a weak source. These results are reported in Chapter 3. Also in Chapter 3, a similar analysis will consider two of the criticality incidents briefly outlined in Table 1.1, to verify the consistency of these results with the CRAC analysis. The results of the KEWB program of Atmoics International (1956 - 66) are also examined.

Hansen has shown that the basis for the possible differences between having a "standard kinetics" response or a "delayed burst" are due to the basic physics parameters, ramp rate and source strength. Using the theory presented in Chapter 2, the validity of this reasoning will be tested through an analysis of the CRAC "delayed burst" experiments. using a report provided by Lécorché and Seale (1973). Therefore, our interests are in both the "weak source" and the "strong source" cases, and in the criterion that differentiates the two. Moreover, it will be shown that the probability of obtaining enough reactivity to cause a high yield burst criticality accident is dependent on the inherent neutron source strength and the rate of reactivity addition.

In March 1975, a study of the potential for a criticality accident in one of the Allied General Nuclear Services

large dissolver tanks was undertaken. These dissolver tanks, which were designed for the Barnwell Nuclear Fuel Reprocessing Plant, are ∿80 cm in diameter and ∿485 cm high. Criticality is possible when the tank is filled with the standard 1000 liter solution to a height of 205 cm. Chapter 4 will present an analysis of the potential for one of these tanks to reach prompt critical. Based on anticipated solution density control, batching control of the uranium inventory, and expected absorbing distributed poison concentrations, criticality of the solution is not expected. However, when a second batch of chopped segments of light water reactor fuel are added to the solution, and the concentration of the dissolved poison is allowed to drop to zero, a critical solution may supervene. The consequences of this double contingency failure was analyzed by Verdon (1975).

CHAPTER 2

THEORY

Consider a supercritical system having simple, finite geometry. For example, the prototype fast-burst reactor GODIVA and other similar systems, when operated in a pulsed fashion, offer the potential for the classic example of the assembly of a reactor in the presence of a weak source. This reactor type uses highly enriched (usually 93%) solid uranium metal as fuel. In this classic case, the metal components were brought rapidly to a configuration that was about 8.5 cents above prompt critical with only the inherent spontaneous fission source present. A burst results which is reproducible in the number of fissions and in width, but is not reproducible as to the time after the assembly for an occurrence of its peak power.

To evaluate the consequences of the assembly of a supercritical system in the presence of a weak and fluctuating source, the distribution between the neutron-induced finite fission chains and the neutron-induced persistent (nonfinite) fission chains must be determined. It is assumed that the additional fluctuations inherent in the growth of the neutron population associated with the persistent fission chains can

be neglected. With this in mind, and for the weak source condition and the small excess reactivity often associated with criticality accidents, approximate equations for the probability distribution in time of a first fission burst have been derived by Hansen. The material that follows is based on Hansen's analysis of this problem. However, before this can be done, it is instructive to develop a definition for the probability of a source neutron sponsoring a persistent fission chain and to better define a strong and weak source condition.

2.1 The Probability, W, of a Source Neutron Sponsoring a Persistent Fission Chain

In considering a reactive system that is supercritical, the assumption will be made that all neutrons behave identically. That is to say, that all neutrons have the probability p of producing a fission, and each fission has the probability $P(\nu)$ of emitting ν neutrons.

Define W_f as the probability of a source fission sponsoring a persistent fission chain, such that $(1-W_f)$ is the probability that a source fission does not sponsor a persistent fission chain. The probability of a source fission not sponsoring a persistent fission chain is equal to the probability that none of its emitted neutrons sponsor such a fission chain. One may then write the following equation:

$$(1-W_f) = \sum_{\nu=0}^{N} P(\nu)\,(1-pW_f)^{\nu} \qquad (2.1)$$

$P(\nu)$ is a known distribution for many fissionable materials and therefore, Eq. (2.1) may be evaluated for $W = pW_f$ in terms of p. For a slightly supercritical system where $W < 1$, the quantity $(1-pW_f)^{\nu}$ may be approximated using a binomial expansion

$$(1-pW_f)^{\nu} \approx 1-\nu pW_f + \frac{\nu(\nu-1)}{2}\,p^2{W_f}^2 \qquad (2.2)$$

Define

$$\bar{\nu} = \sum_{\nu=0}^{\nu} \nu P(\nu) \qquad (2.3)$$

as the average value of the number of neutrons emitted per fission, and obtain for $W << 1$:

$$(1-W_f) \approx 1 - \bar{\nu}pW_f + \overline{\nu(\nu-1)}\,\frac{p^2{W_f}^2}{2} \qquad (2.4)$$

The quantity $\bar{\nu}p$ is the average number of daughter fissions produced per fission, and is conventionally referred to as the reproduction number k. Using this notation together with Γ_2 defined as

$$\Gamma_2 = \frac{\overline{\nu(\nu-1)}}{\bar{\nu}^2} \qquad (2.5)$$

Eq. (2.4) may be re-expressed as:

$$pW_f \approx \frac{2(k-1)}{\overline{\nu(\nu-1)}p} = \frac{2\delta k}{\overline{\nu}\Gamma_2} \tag{2.6}$$

where it should be noted that since $W << 1$, $\overline{\nu}p \approx 1$. Finally, noting that $\delta k = k-1$

$$W = \frac{2\delta k}{\overline{\nu}\Gamma_2} \qquad \text{for } 0<\delta k<<1$$

$$W = 0 \qquad \text{for } \delta k<0 \tag{2.7}$$

2.2 The Definition of a Strong and Weak Neutron Source

Consider now a neutron source in the reacting system of strength S neutrons per second. The expected number of persistent fission chain initiations per second is then $W \cdot S$ and hence the average time interval between successive initiations is simply $1/W \cdot S$.

The expected growth in neutron population associated with the i^{th} persistent fission chain, $n_i(t)$, is of the form

$$Ae^{\delta k(t-t_i)/\tau} \tag{2.8}$$

where A is just a normalization constant and τ is the mean neutron lifetime. The expected value of $n_{i+1}(t)$ is then

$$n_i(t)e^{-\delta k/WS\tau} \tag{2.9}$$

and if the argument of the exponential is much greater than unity, the total neutron population at time t would essentially be comprised of neutrons associated with the first persistent fission chain. This defines the weak source condition, since using Eq. (2.7) for $0 < \delta k << 1$, W may be eliminated, and the condition $\delta k/WS\tau >> 1$ becomes

$$\frac{2S\tau}{\bar{\nu}\Gamma_2} << 1 \tag{2.10}$$

which is the definition of a weak source.

When $S\tau >> 1$, a strong source condition exists and the neutron population at a time after assembly, $t >> \tau/\delta k$, is derived from source neutrons occurring in the first e-folding time, $t_1 = \tau/\delta k$.

During the interval t_1, the expected number of persistent fission chains being sponsored is

$$\bar{N} = WSt_1 = \frac{2S\tau}{\bar{\nu}\Gamma_2} \tag{2.11}$$

and the probability distribution in N is Poisson, such that

$$\frac{1}{\bar{N}} = \frac{(\overline{N^2} - \bar{N}^2)}{\bar{N}^2} \tag{2.12}$$

Therefore, the fluctuation in neutron population, n(t), is accordingly

$$\frac{\overline{[n(t)^2 - \bar{n}(t)^2]}}{\bar{n}(t)^2} \sim \frac{\bar{\nu}\Gamma_2}{2S\tau} \qquad (2.13)$$

It should be noted that the fluctuations in neutron population buildup associated with a single persistent fission chain has been neglected. The fluctuation in time at which the neutron population reaches some moderately large value is then given by

$$\frac{(\delta k)^2 \ (\overline{t^2} - \bar{t}^2)}{\tau^2} \sim \frac{\bar{\nu}\Gamma_2}{2S\tau} \qquad (2.14)$$

In the weak source case, fluctuations in time up to a prescribed power level are even larger than suggested by the above 1/S proportionality.

2.3 The Probability Distribution in Time of the Occurrence of a Fission Burst Following a Ramp Increase of Reactivity

It is convenient to set up and illustrate a coordinate system in time that is directly related to the following derivation; this is illustrated in Figure 2.1.

The instant the system becomes prompt critical, $t = 0$. The time t represents the occurrence of the fission burst and is composed of two parts: $t = t_1 + t_2$. t_1 represents the time at which the first persistent fission chain is sponsored, and t_2 the time for the neutron population associated with this fission chain to grow to a maximum. Figure 2.1 illustrates

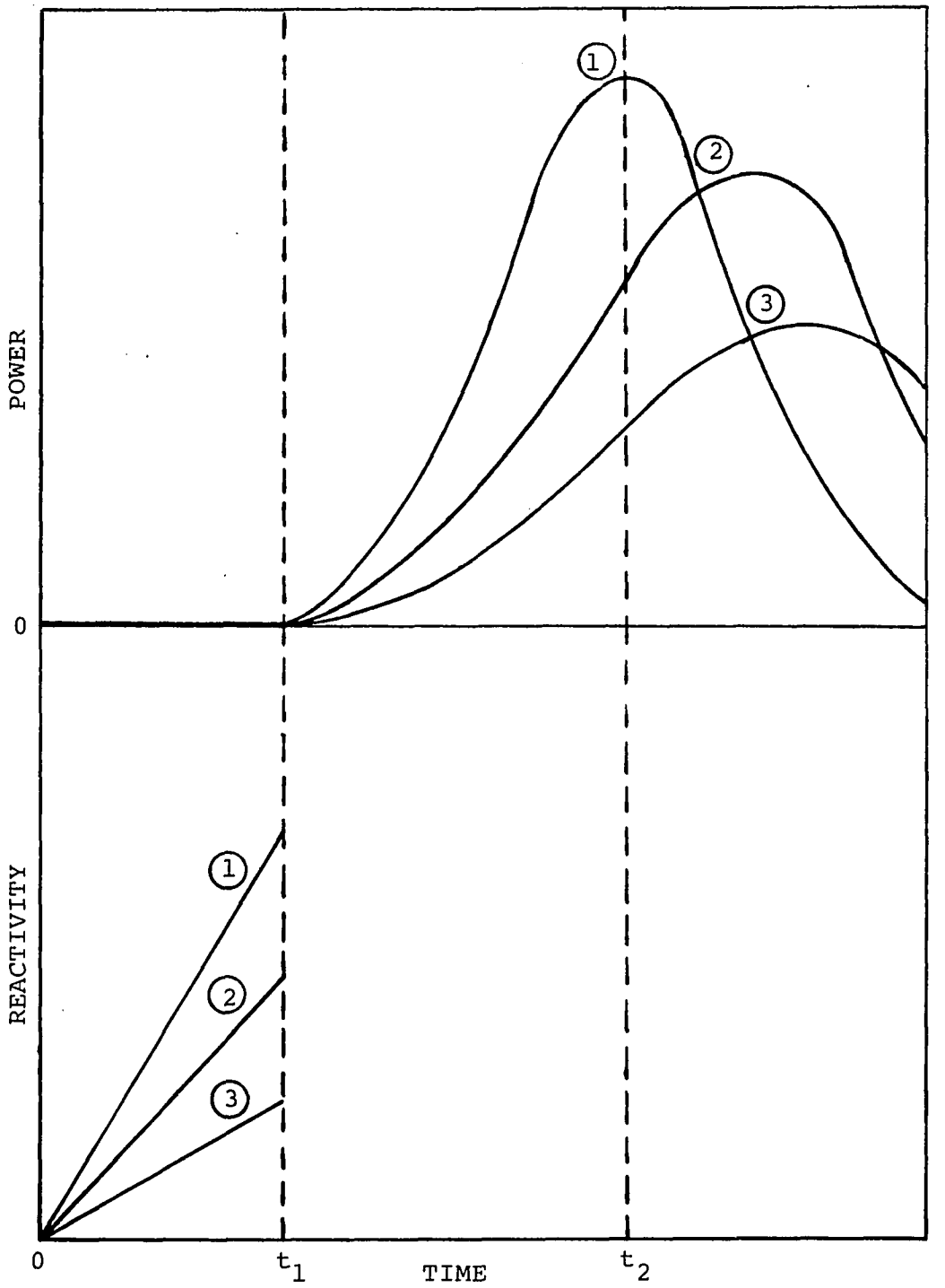

Figure 2.1. Power and reactivity vs time.

how the ramp rate influences the growth of the neutron population.

During the initial growth period prior to the onset of any feedback mechanisms, and neglecting delayed neutrons, the time dependence of the neutron population is governed by the following kinetics equation:

$$\frac{d\bar{n}(t)}{dt} = \left(\frac{\rho}{\tau}\right)\bar{n}(t) + S \qquad (2.15)$$

where $\rho = at$ for a constant ramp reactivity increase, and S is some external source strength. A solution to this equation may be obtained using an integral factor of the form $\exp(-at^2/2\tau)$:

$$\bar{n}(t) = e^{at^2/2\tau} \int_{-\infty}^{t} S\, e^{-at'^2/2\tau}\, dt' \qquad (2.16)$$

The lower limit of the integral was chosen since source fissions occurring prior to $t' = 0$ are responsible for one-half of the average asymptotic neutron population. Upon integration, and for $t >> (2\tau/a)^{\frac{1}{2}}$:

$$\bar{n}(t) \approx \sqrt{\frac{2\pi S^2 \tau}{a}}\; e^{at^2/2\tau} \qquad (2.17)$$

Eq. (2.17) is the average asymptotic neutron population and indicates that persistent fission chains sponsored prior to the system reaching critical, play an important role in

determining n(t). It should be noted that Eq. (2.17) is not an exact solution to Eq. (2.15), yet it is a good approximation and clearly illustrates the behavior of the average neutron population.

Thus far the reproduction number, k, has not been treated as a function of time. For a time-dependent reproduction number, the quantity pW_f appearing in the right-hand sides of Eqs. (2.1) and (2.2) must be generalized to

$$\frac{1}{\bar{\nu}} \int_t^\infty k(t')W_f(t') \frac{e^{-(t-t')/\tau}}{\tau} dt' \qquad (2.18)$$

which indicates that a neutron emitted by a source fission at time t is absorbed at a later time t' with a probability $e^{-(t'-t)/\tau}dt'/\tau$. As before, neglecting terms higher than W_f^2, Eq. (2.4) becomes for $W << 1$:

$$W_f \approx \bar{\nu}pW_f - \frac{}{\nu(\nu-1)} \frac{p^2 W_f^2}{2} \qquad (2.19)$$

Replacing the quantity pW_f in Eq. (2.19) with Eq. (2.18), W_f then becomes a function of time, $W_f(t)$. Using Leibniz' Theorem to take the derivative with respect to time of the resulting equation, a first order non-linear differential equation results:

$$\frac{dW_f(t)}{dt} + \frac{\delta k(t)}{\tau} W_f(t) = \frac{\Gamma_2}{2\tau} W_f(t)^2 \qquad (2.20)$$

The form of this equation is called a Bernoulli Differential Equation, and may be reduced to a linear equation by making the transformation $v(t) = W_f(t)^{-1}$. The solution to the resulting linear equation can then be obtained using an integrating factor of the form $\exp\left(-\int_t^{t'} \delta k(t'')dt''/\tau\right)$:

$$W_f(t) = \exp\left(\int_t^{t'} \frac{\delta k(t'')}{\tau}\, dt''\right) \cdot \left[\frac{\Gamma_2}{2\tau}\int_t^{\infty} \exp\left(-\int_t^{t'} \frac{\delta k(t'')}{\tau}\, dt''\right) dt'\right] \tag{2.21}$$

For $\delta k(t\to\infty)>0$, and noting that $W(t) = pW_f(t)$

$$W(t) = \frac{2\tau}{\bar{\nu}\Gamma_2 \int_t^{\infty} \exp\left(-\int_t^{t'} \frac{\delta k(t'')}{\tau}\, dt''\right) dt'} \tag{2.22}$$

For the ramp, $\delta k(t) = at$, Eq. (2.22) reduces to

$$W(t) = \frac{2\tau}{\bar{\nu}\Gamma_2 \exp\left(\frac{at^2}{2\tau}\right)\left(\frac{2\tau}{a}\right)^{1/2}\int_{\sqrt{\frac{a}{2\tau}}\,t}^{\infty} e^{-z^2}\, dz} \tag{2.23}$$

Upon further simplification and knowing the definitions of the error function:

$$W(t) = \frac{\sqrt{8a\tau/\pi\bar{\nu}^2\Gamma_2^2}\ \exp(-at^2/2\tau)}{1 - \operatorname{erf}(\sqrt{a/2\tau}\,t)} \qquad (2.24)$$

W(t) represents the probability as a function of time, of the occurrence of a source neutron sponsoring a persistent fission chain following a ramp increase of reactivity.

The probability of the first persistent fission chain being sponsored at time t_1 in the interval dt_1 is

$$P(t_1)dt_1 = \exp\left[-\int_{-\infty}^{t_1} W(t')Sdt'\right] W(t_1)Sdt_1 \qquad (2.25)$$

Substitution of W(t′) from Eq. (2.24) into the argument of the exponential in Eq. (2.25) yields

$$\exp\left[-\sqrt{\frac{8a\tau S^2}{\pi\bar{\nu}^2\Gamma_2^2}}\int_{-\infty}^{t_1}\left\{\operatorname{erfc}\left(\sqrt{\frac{a}{2\tau}}\,t'\right)\right\}^{-1} e^{-\frac{at'^2}{2\tau}}\,dt'\right] \qquad (2.25a)$$

remembering that erfc(z)=1-erf(z). Then, after making a change in variables, the integral can be expressed in the form of an exact integral, which yields a solution, $-(\pi\tau/2a)^{\frac{1}{2}}\ln(\operatorname{erfc}(\sqrt{a/2\tau}t_1)/2)$. Eq. (2.25a) then becomes

$$\exp\left(\frac{2S\tau}{\bar{\nu}\Gamma_2}\ln\frac{\operatorname{erfc}\left(\sqrt{\frac{a}{2\tau}}\,t_1\right)}{2}\right)=\left(\frac{\operatorname{erfc}\left(\sqrt{\frac{a}{2\tau}}\,t_1\right)}{2}\right)^{\frac{2S\tau}{\bar{\nu}\Gamma_2}} \tag{2.25b}$$

Substituting $W(t_1)$ from Eq. (2.24) and the result of Eq. (2.25b) into Eq. (2.25), a final expression for $P(t_1)dt_1$ is:

$$P(t_1)dt_1=\sqrt{\frac{2a\tau S^2}{\pi\bar{\nu}^2\Gamma_2^2}}\left(\frac{1-\operatorname{erf}\left(\sqrt{\frac{a}{2\tau}}\,t_1\right)}{2}\right)^{\frac{2S\tau}{\bar{\nu}\Gamma_2}-1}e^{-at_1^2/2\tau}dt_1 \tag{2.25c}$$

For various source strengths, $2S\tau/\bar{\nu}\Gamma_2$, this equation yields a probability distribution for the first persistent fission chain sponsored at time t_1 in the interval dt_1.

In the case of a weak source condition, $P(t_1 < 0)$ is very small, thus indicating that persistent fission chains sponsored prior to the system reaching critical play an unimportant role in determining $\bar{t}_1$ and hence the average time $\bar{t} = \bar{t}_1+\bar{t}_2$ for the neutron population to reach an established level. For a strong source condition, the situation is reversed. Persistent fission chains sponsored prior to the system reaching criticality play a significant role in determining $\bar{t}_1$ and hence $\bar{t}$.

For the weak source condition alone, an approximation of Eq. (2.25c) may be obtained by representing $W(t)$ by $2\delta k(t)/\bar{\nu}\Gamma_2$ for $t > 0$. Upon substitution of $W(t')$ and $W(t_1)$

into Eq. (2.25) and letting $\delta k(t) = at$ for a constant ramp increase of reactivity, one obtains for $t_1 \geq 0$

$$P(t_1)dt_1 \cong \frac{2aSt_1}{\bar{\nu}\Gamma_2} \cdot e^{-aSt_1^2/\bar{\nu}\Gamma_2} \, dt_1 \qquad (2.26)$$

Eq. (2.25c) is valid for all values of t_1, whereas in this instance, $P(t_1) = 0$ for $t_1 < 0$ since $W(t) = 0$ for $t < 0$. It is important to note that this approximation of $W(t)$ is not suitable for estimations of $\bar{n}(t)$ or $\overline{n(t)^2}$ and hence the fluctuation in neutron population, $n(t)$.

2.4 Summary

In concluding Chapter 2, it may be instructive to summarize the results obtained thus far.

The first development of this chapter was an equation for the probability, W, of a source neutron sponsoring a persistent fission chain, and a distinction was made between W and W_f, the probability of a source fission sponsoring a persistent fission chain. Next, the conditions for having a strong or a weak neutron source were defined, and Eqs. (2.13) and (2.14) described the fluctuation in neutron population. It was then realized in the weak source case, where most of our attention is focused, fluctuations in time up to a prescribed power level are even larger than suggested by the 1/S proportionality. A coordinate system in time was then

set up which defined t = 0 as the instant the system becomes prompt critical.

Then, during the neutron population's initial growth period, the kinetics equation, Eq. (2.15), governing this period was solved for a constant ramp of reactivity increase. For $t >> (2\tau/a)^{\frac{1}{2}}$, Eq. (2.17) is an approximate solution to Eq. (2.15), and illustrates that persistent fission chains sponsored prior to the system reaching prompt critical play an important role in determining the fluctuation in neutron population, n(t).

Our attention was then directed to treating the reproduction number, k, as a function of time thereby generalizing the quantity pW_f and forcing W to become a function of time, W(t). This was given by Eq. (2.24), which represents the probability as a function of time of the occurrence of a source neutron sponsoring a persistent fission chain following a ramp insertion of reactivity. Using this result, and an expression for the probability of the first persistent fission chain being sponsored at time t_1 in the interval dt_1, a final expression, Eq. (2.25c), was given which will be used at a later time. This equation is unique in that it is a function of source strength, and is valid for all values of t_1. For the weak source condition alone, an approximation to Eq. (2.25c) was obtained by representing W(t) by

$2\delta k(t)/\bar{\nu}\Gamma_2$ for $t > 0$. This expression, Eq. (2.26), is only valid for $t_1 \geq 0$ and is zero otherwise.

In Chapter 3 actual experiences with solutions, present examples of a weak source condition, in which Eq. (2.26) will be used, whereas in Chapter 4, the AGNS dissolver tank will be an example of a strong source condition and will employ Eq. (2.25c). It is important to note that Hansen's analysis is <u>not</u> sufficient for systems in which delayed neutrons are involved.

CHAPTER 3

ACTUAL EXPERIENCE WITH CRITICAL SOLUTIONS

To date, there have been eight supercritical accidents involving chemical process equipment and none associated with mechanical processing, storage, or transportation. Each incident was the result of process or equipment difficulty or maloperation, or both. All occurred with aqueous solutions; five involved highly enriched uranium, and three involved plutonium. Even though there was at no time any danger to the general public, these excursions are regarded as dangerous because for extreme cases, the exponential rise of power is so rapid that safety devices cannot react in time to prevent damage to the system and irradiation to personnel. Some of these excursions have been terminated by the operation of safety devices while others have terminated by natural quenching mechanisms that are roughly proportional to the fission energy that has been generated.

A comprehensive understanding of the parameters of importance in criticality accidents may be based on reasonably simple analytical models, with the accidents listed in Table 1.1 as valuable "bench marks" that generally confirm these models. In 1968, a systematic experimental study of

the results of deliberate accumulations of supercritical amounts of fissionable material as an aqueous solution was launched by the French CEA. The CRAC (Consequences Radiologiques d' un Accident de Criticité) experiment results gave valuable insight into the behavior expected in accidental supercritical accumulations that may occur in chemical processing.

Within the details of the CRAC experiments, there is data that can be analyzed to demonstrate the importance of source strength and the rate of reactivity addition on the yields from delayed bursts. These results should provide a quantitative insight into the extent to which these parameters can be useful in design for accident mitigation or prevention.

3.1 The CRAC Experiments

In this program, a series of experiments were performed in which 93% enriched aqueous uranyl nitrate solutions at various concentrations were injected into large cylinders to heights in excess of the critical height. Altogether, there are fifty-eight CRAC experiments and eleven "slow excursion" experiments. The "slow excursion" experiments are a series of stable reactor period measurements made for a fixed, slightly supercritical, volume of solution at a given concentration. These measurements allow direct determination of the reactivity worth of incremental additions

of solution to a critical volume for various uranium solution concentrations.

The CRAC experiments, performed without an external source present, and having an initial subcritical volume of solution, are worthy of special analysis. There were twenty-nine experiments in which the only neutron sources were due to spontaneous fission and (α,n) reactions on oxygen. Table 3.1 lists these experiments along with their detailed experimental parameters; i.e., concentration, critical volume, and neutron source strengths. CRAC-01 through -29 are 300 mm diameter cylinders, and CRAC-37 through -43 are 800 mm diameter cylinders.

The normal experimental procedure was to inject solution into the cylinder at a constant volume rate resulting in an initially uniform ramp-rate increase in reactivity. After a supercritical volume of solution had accumulated in the cylinder and a neutron had induced the first persistent chain, the power increased to a peak, which corresponded to the power at which heating and radiolytic gas formation resulted in a decreased density, adequate to provide an override of the excess reactivity. The initial pulse died out as expansion reduced the reactivity below the critical condition, terminating gas generation momentarily. The solution drained to the bottom of the tank as bubbles escaped, and the reactivity again rose above the critical value. A second pulse

Table 3.1. Spontaneous fission source strengths for twenty-nine CRAC experiments.

Exp. No.	Uranium Conc (gms/liter)	U-235 Conc (gms/liter)	Critical Volume (liters)	SF Source Strength (neutrons/sec)	(α,n) Source Strength (neutrons/sec)
CRAC-01	52.0	48.4	129.8	6.3	520
CRAC-03	52.2	48.6	123.5	6.0	497
CRAC-04	51.7	48.2	131.5	6.3	524
CRAC-05	61.1	56.9	47.1	2.7	221
CRAC-06	61.1	56.9	46.5	2.6	218
CRAC-07	202	188	18.7	3.5	283
CRAC-08	202	188	18.9	3.5	287
CRAC-09	78.3	72.9	29.5	2.1	177
CRAC-10	78.3	72.9	29.3	2.1	176
CRAC-12	77.9	72.5	29.9	2.2	179
CRAC-13	77.9	72.5	33.5	2.4	200
CRAC-19	82.0	76.4	28.5	2.2	179
CRAC-20.4	218	203	18.8	3.8	307
CRAC-20.5	218	203	18.8	3.8	307
CRAC-21	80.2	74.7	28.7	2.1	177
CRAC-22	207	193	18.6	3.6	289
CRAC-23	91.8	85.5	25.5	2.2	179
CRAC-25	320	298	19.0	5.7	448
CRAC-26	165.9	154.5	19.7	3.0	247
CRAC-27	89.0	82.9	26.4	2.2	180
CRAC-28	89.0	82.9	26.4	2.2	180
CRAC-29	81.0	75.4	29.1	2.2	181
CRAC-37	21.8	20.3	221.9	4.5	375
CRAC-38	21.4	19.9	230.5	4.6	383
CRAC-39	30.6	28.5	134.4	3.8	318
CRAC-40	58.7	54.7	92.0	5.0	416
CRAC-41	59.3	55.2	91.4	5.0	417
CRAC-42	203	189	71.8	13.6	1094
CRAC-43	202	188	70.9	13.4	1075

then occurred similar to the first, and so on through a series of pulses. In all the experiments, solution was added through the duration of the first peak and, in many cases, was continued until several peaks were observed. Eventually, fissions generated in the solution caused heating, and in some cases, some material ejection and gas formation which compensated for the excess reactivity originating from the excess fuel initially added, and a constant power was achieved. Of particular interest are the parameters that describe the first peak in the pulse chain, including the role of source strength and reactivity ramp rate as they relate to the beginning of the first persistent fission chain.

This may be determined for each of the CRAC experiments by evaluating the quantity $2S\tau/\bar{\nu}\Gamma_2$ previously derived in Chapter 2. Table 3.1 lists the calculated source strength, S, due to spontaneous fission and (α,n) reactions for each of the CRAC experiments. For these small-sized cylinders, leakage of neutrons is significant and an effective source strength should be determined. This is achieved through the use of the following equation

$$S_{eff} \cong \frac{S}{1 + M^2B^2} \tag{3.1}$$

The thermal migration area, M^2, may be determined using the critical equation, namely

$$M^2 = \frac{k_\infty - 1}{B^2} \qquad (3.2)$$

which is the critical equation from modified one-group theory. The four data points shown in Figure 3.1 are provided from a memo by F. Y. Barbry (1976). These data are listed below in Table 3.2:

Table 3.2. Data for Figure 3.1.

Uranium Conc (gms/liter)	Migration Area (mm^2)	Buckling Geometric x $10^{-4} mm^{-2}$	k_∞
60.9	2240	2.00	1.448
101.4	2170	2.37	1.514
146.3	2120	2.66	1.563
220.0	2210	2.75	1.607

where k_∞ was calculated, knowing the geometric buckling corresponding to each of the four uranium concentrations at the critical condition; i.e., $k_\infty = 1 + M^2B^2$. Figure 3.2 was generated using the following equation:

$$B^2 = \left(\frac{2.405}{r + \lambda_{ext}} \right)^2 + \left(\frac{\pi}{h + 2\lambda_{ext}} \right)^2 \qquad (3.3)$$

where λ_{ext} is an extrapolation length for the fuel. It was found that a value of 28 mm for λ_{ext} resulted in a consistent fit for the 300 mm and 800 mm cylinder data.

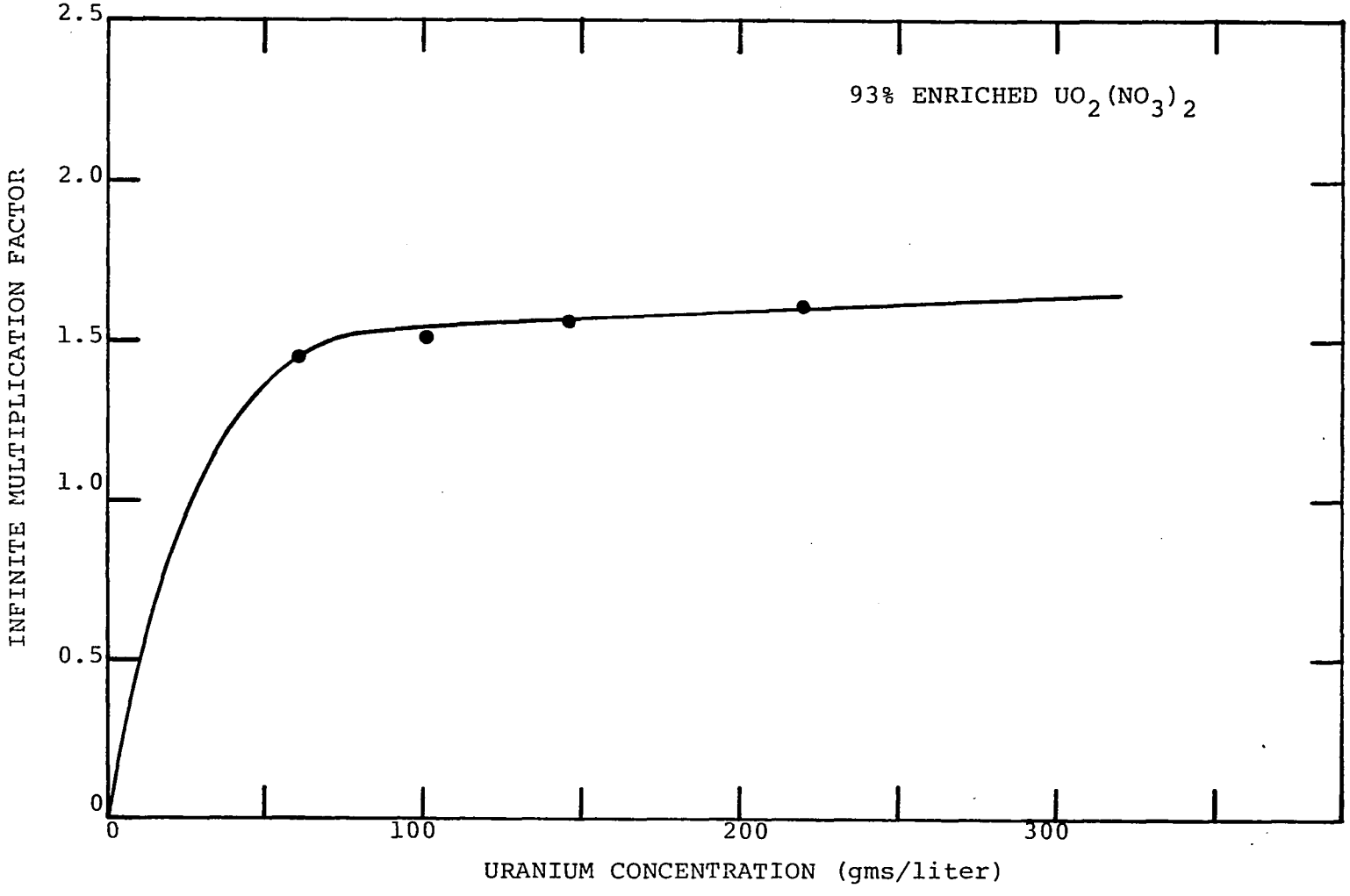

Figure 3.1. Infinite multiplication factor vs uranium concentration.

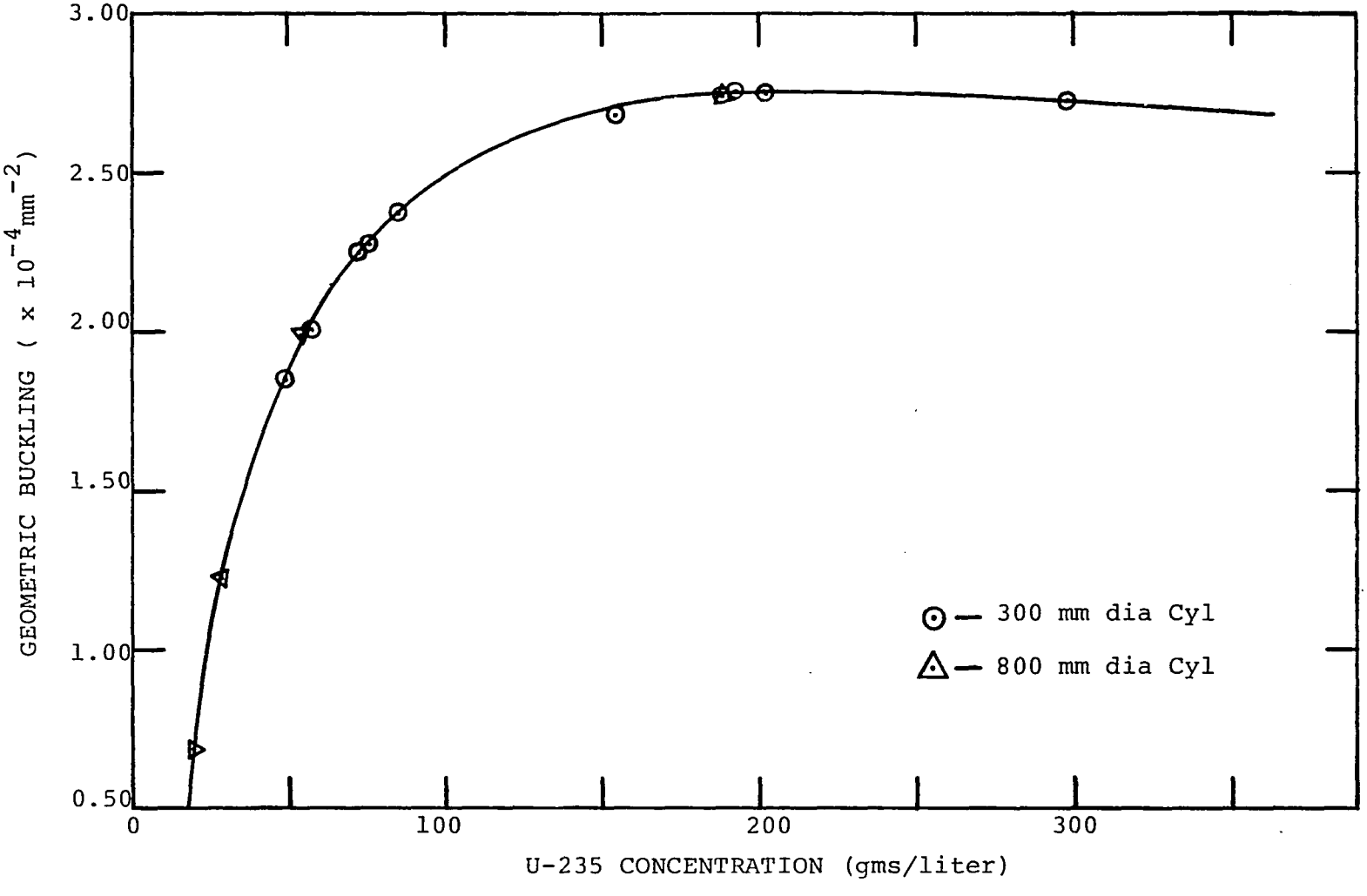

Figure 3.2. Geometric buckling vs U-235 concentration.

The neutron lifetime, τ, is determined from Figure 3.3 knowing the U-235 concentration for each CRAC experiment. The twelve data points illustrated in Figure 3.3 are provided from actual measurements during the experiments, and are listed in Table 3.3. The infinite multiplication factor, k_∞, is determined from Figure 3.1 knowing the uranium concentration, and the geometric buckling, B^2, is determined from Figure 3.2 knowing the U-235 concentration, for each of the CRAC experiments. Using Eq. (3.2) the migration area may then be determined for each of the CRAC experiments.

Table 3.3. Data for Figure 3.3.

Experiment Number	U-235 Conc (gms/liter)	Neutron Lifetime (μsec)
CRAC-01	48.4	41
CRAC-05	56.9	37
CRAC-07	188	13.5
CRAC-09	72.9	31
CRAC-20.4	203	13
CRAC-22	193	13
CRAC-23	85.5	26
CRAC-26	154.5	15.7
CRAC-27	82.9	27
CRAC-37	20.3	74
CRAC-39	28.5	61
CRAC-40	54.7	38

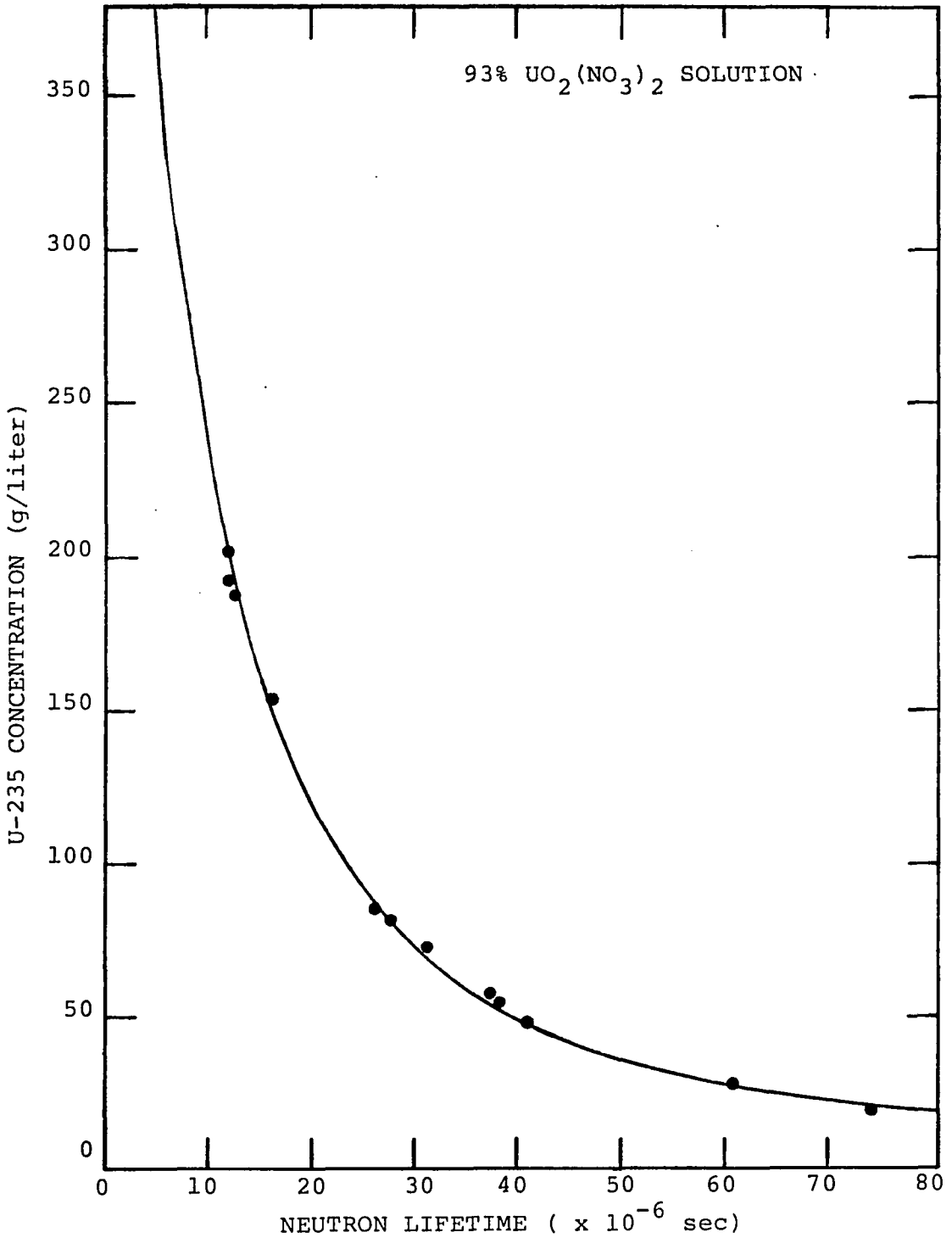

Figure 3.3. U-235 concentration vs neutron lifetime.

The quantities $\bar{\nu}$ and Γ_2 previously defined in Chapter 2 were determined from Lamarsh (1972) and Terrell (1957) respectively, and it was found that the values $\bar{\nu} = 2.44$ neutrons per fission and $\Gamma_2 = 0.8$ are appropriate.

The source condition for each of the CRAC experiments may now be determined and Table 3.4 lists these results. Recall from Chapter 2 that according to Hansen, for the condition $2S\tau/\bar{\nu}\Gamma_2 << 1$, the source strength is judged weak. Table 3.4 indicates that for the majority of the twenty-nine CRAC experiments this quantity is on the order of 10^{-3}, and hence the weak source condition is satisfied.

As solution is injected into the cylinders at a constant rate, reactivity initially increases linearly with height above delayed critical. Except for three experiments, this reactivity increase remains fairly linear until the final volume is reached. In CRAC-01, -03, and -04 reactivity increases with height in a nonlinear fashion as illustrated in Figure 3.4. The 800 mm diameter cylinders have a greater degree of linearity than the majority of the 300 mm diameter cylinders, due to their larger diameter. In these experiments there is a smaller increase in height needed in reaching the final volume, and Figure 3.5 illustrates this reactivity change with height for the 800 mm diameter cylinders. Appendix A presents a one-group reactivity analysis, and the equations from which these two figures were developed.

Table 3.4. Source condition for twenty-nine CRAC experiments.

Exp. No.	Migration Area (mm^2)	Buckling Geometric ($\times 10^{+4} mm^{-2}$)	Effective Source Strength (neutrons/sec)	Neutron Lifetime (μsec)	$\frac{2S_{eff}\tau}{\overline{\nu}\Gamma_2} \times 10^{+3}$
CRAC-01	2190	1.85	375	41	15.7
CRAC-03	2185	1.85	360	41	15.0
CRAC-04	2190	1.85	380	41	15.9
CRAC-05	2245	2.00	155	37	5.9
CRAC-06	2240	2.01	155	37	5.8
CRAC-07	2180	2.75	180	13.5	2.5
CRAC-08	2190	2.74	180	13.5	2.5
CRAC-09	2140	2.24	120	31	3.8
CRAC-10	2135	2.25	120	31	3.8
CRAC-12	2150	2.23	120	31	3.9
CRAC-13	2225	2.16	140	31	4.3
CRAC-19	2140	2.27	120	28.7	3.6
CRAC-20.4	2220	2.75	195	13	2.6
CRAC-20.5	2220	2.75	195	13	2.6
CRAC-21	2135	2.26	120	29.5	3.6
CRAC-22	2195	2.76	180	13	2.4
CRAC-23	2110	2.37	120	26	3.2
CRAC-25	2475	2.73	270	10.7	3.0
CRAC-26	2145	2.68	160	15.7	2.5
CRAC-27	2120	2.34	120	27	3.4
CRAC-28	2120	2.34	120	27	3.4
CRAC-29	2145	2.25	125	29.3	3.7
CRAC-37	428	0.70	370	74	27.9
CRAC-38	148	0.68	385	74	29.1
CRAC-39	1380	1.23	275	61	17.2
CRAC-40	2190	1.99	295	38	11.4
CRAC-41	2195	2.01	295	38	11.4
CRAC-42	2197	2.74	690	13	9.2
CRAC-43	2150	2.79	680	13	9.1

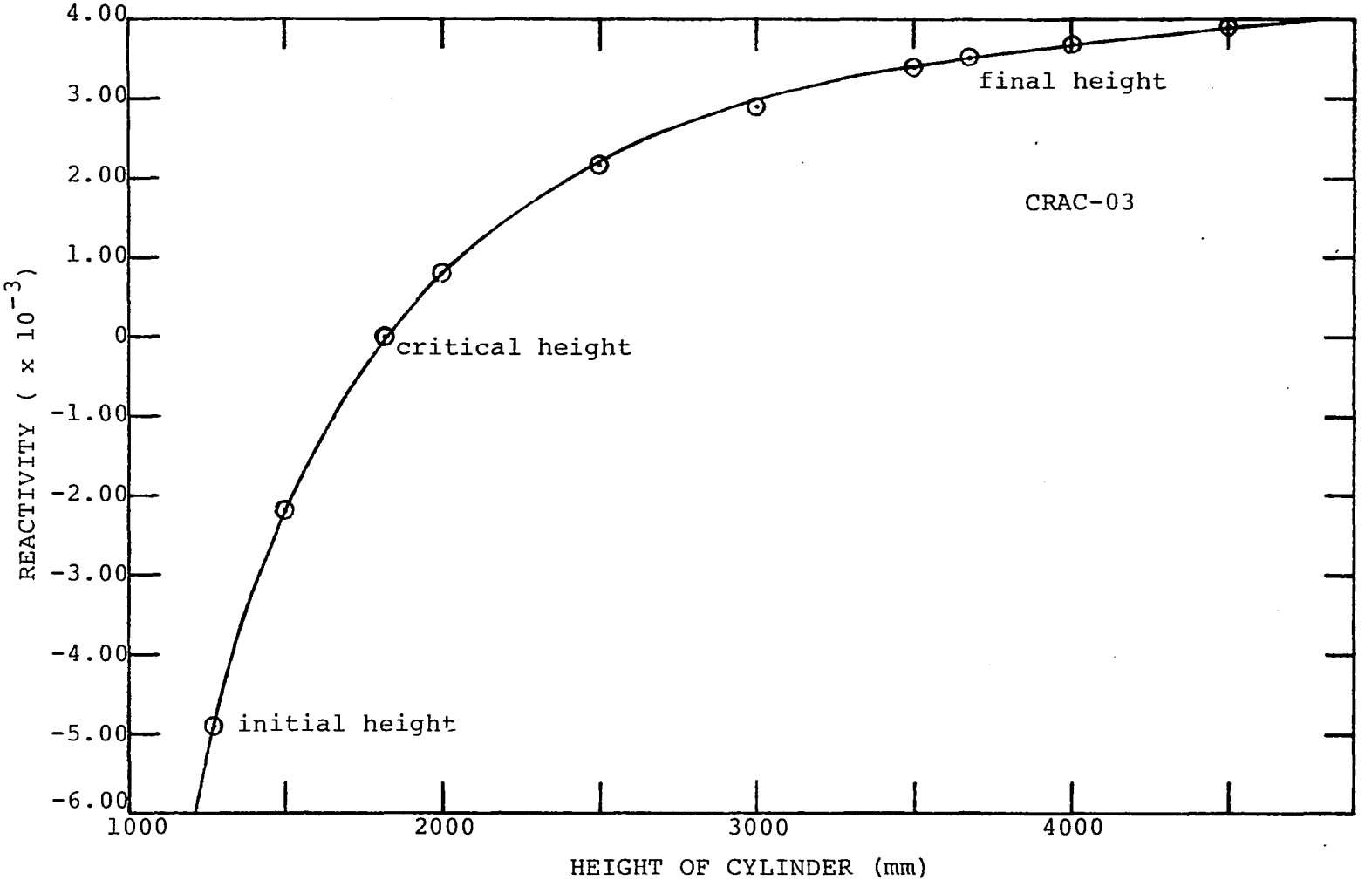

Figure 3.4. Reactivity vs height of 300 mm dia cylinder.

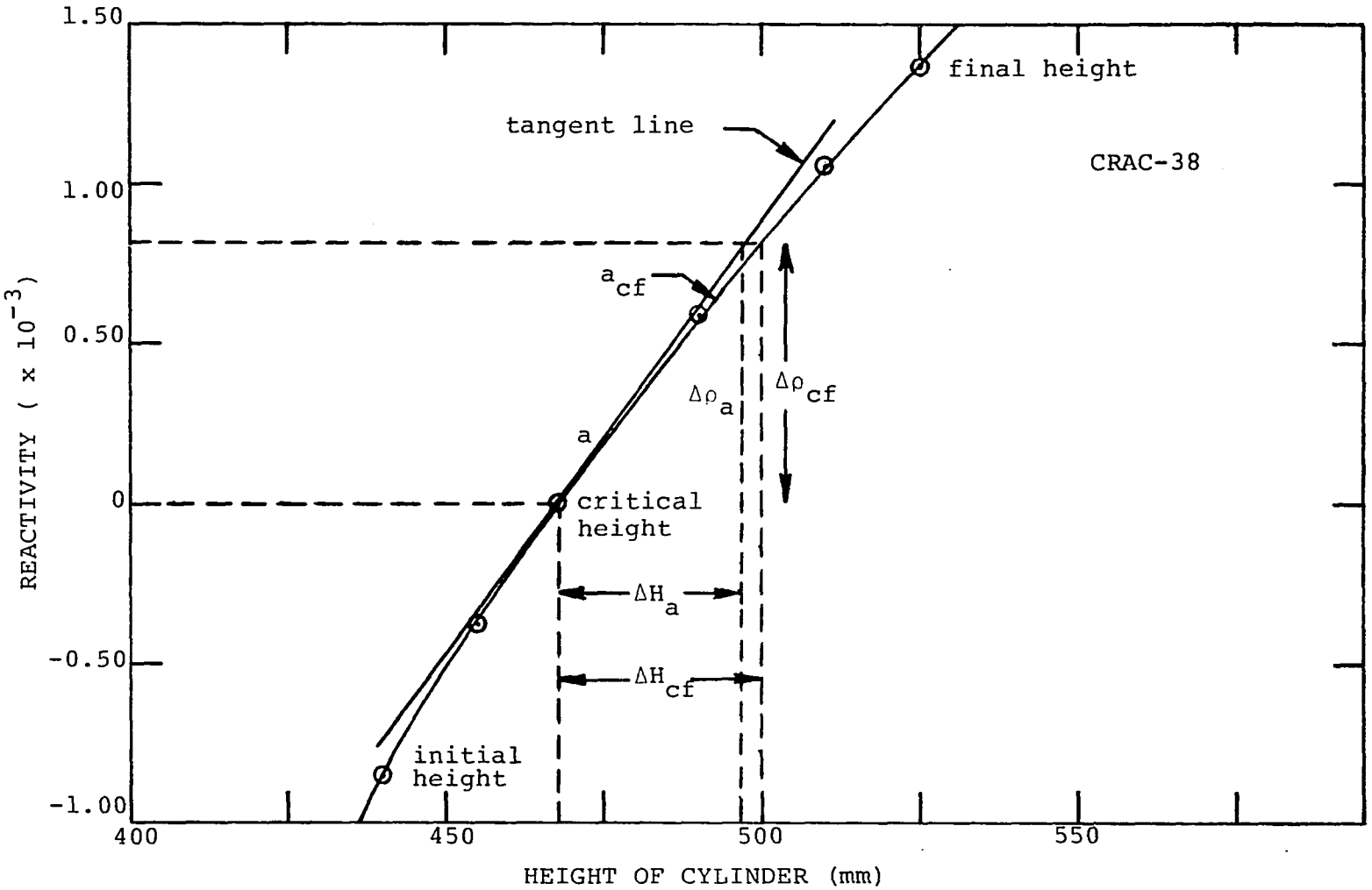

Figure 3.5. Reactivity vs height of 800 mm dia cylinder.

Knowing the ramp rate of reactivity addition, and using Eq. (2.26), the probability of the first persistent fission chain being sponsored at time t_1 may be obtained. Figure 3.6 shows this probability and represents an ensemble of CRAC experiments. It is seen that the probability for $t_1 < 0$ is very small, indicating that persistent fission chains sponsored prior to the system reaching critical play an unimportant role in determining the average time for the neutron population to reach a prescribed value. This is only true for the cases involving a weak source.

The time to the peak of the first burst from delayed critical was determined from the individual CRAC reports and is listed in Table 3.5. Also in Table 3.5 is the reactivity added at the peak of the first pulse, the ramp rates, and the time t_p at which the system went prompt critical for each of the CRAC experiments. The dimensionless time of the first burst $(aS_{eff}/\bar{\nu}\Gamma_2)^{\frac{1}{2}}t$ is also listed. It should be noted that for experiments 25 and 26, a malfunction of recording equipment resulted in a loss of the time record for pulses. In Figure 3.7 $\int_0^t P(t_1)dt_1$ vs $(aS_{eff}/\bar{\nu}\Gamma_2)^{\frac{1}{2}}t$ is plotted and the distribution in time of these fission bursts are positioned below the curve. The time of chain initiation for the CRAC experiments should be clustered in the vicinity of $I(t) = 0.5$. This would indicate that these experiments are located near the top of the probability curve in Figure 3.6. This is the

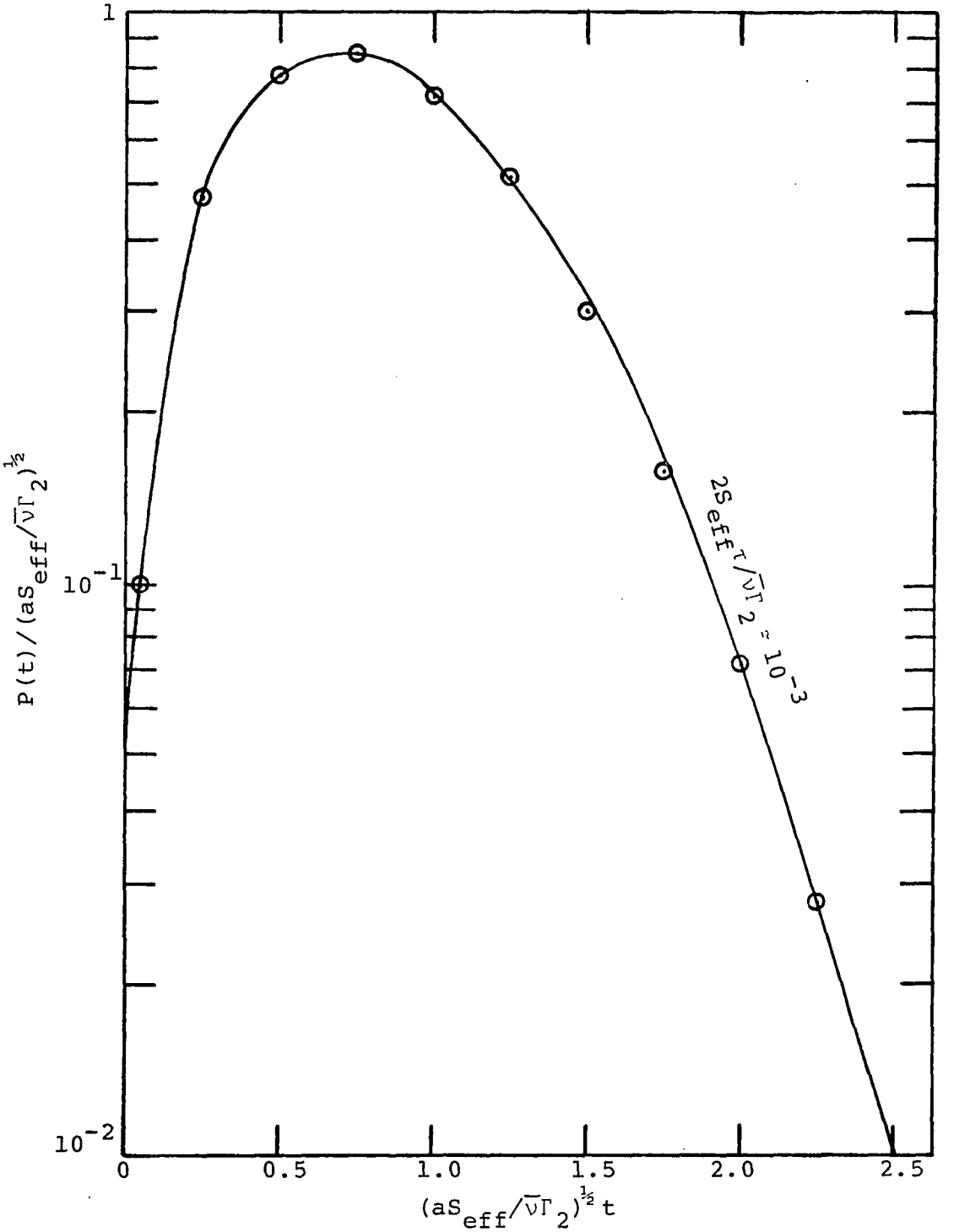

Figure 3.6. Probability of the first persistent fission chain under a ramp insertion.

Table 3.5. Distribution of fission bursts.

Exp. No.	Reactivity Added At Peak of First Pulse (dollars)	Reactivity Addition Rate (dollars/sec)	Time to Peak Of First Pulse (sec)	Time of Prompt Critical (sec)	$\left(\frac{aS_{eff}}{\bar{\nu}\Gamma_2}\right)^{\frac{1}{2}} t$
CRAC-01	0.79	0.00341	232	293.25	- 4.35
CRAC-03	0.60	0.00141	427	709.22	-12.64
CRAC-04	0.77	0.00391	197	255.75	- 4.52
CRAC-05	1.43	0.0667	21.5	14.99	1.31
CRAC-06	1.69	0.0740	22.84	13.51	1.97
CRAC-07	3.06	0.786	3.894	1.272	2.05
CRAC-08	2.31	0.746	3.1	1.34	1.38
CRAC-09	1.58	0.247	6.4	4.05	0.85
CRAC-10	0.51	0.0772	6.62	12.95	- 1.25
CRAC-12	1.01	0.0156	65	64.10	0.08
CRAC-13	1.17	0.157	7.47	6.37	0.33
CRAC-19	1.41	0.0870	16.18	11.49	0.99
CRAC-20.4	2.30	0.685	3.36	1.46	1.43
CRAC-20.5	1.56	0.616	2.53	1.62	0.65
CRAC-21	1.41	0.0833	16.96	12.00	1.01
CRAC-22	2.29	0.501	4.57	2.00	1.61
CRAC-23	1.44	0.310	4.64	3.22	0.56
CRAC-25	4.63	0.871	--	--	--
CRAC-26	5.23	0.638	--	--	--
CRAC-27	1.45	0.315	4.6	3.17	0.56
CRAC-28	1.99	0.226	8.8	4.42	1.49
CRAC-29	0.99	0.0808	12.2	12.38	- 0.04
CRAC-37	0.28	0.00381	72.8	262.47	-13.57
CRAC-38	0.11	0.00368	30.4	271.74	-17.29
CRAC-39	0.15	0.01383	11.0	72.31	- 7.40
CRAC-40	0.61	0.1494	4.1	6.69	- 1.09
CRAC-41	0.87	0.01746	49.7	57.27	- 1.09
CRAC-42	0.55	0.3062	1.8	3.26	- 1.42
CRAC-43	1.08	0.3377	3.2	2.96	0.20

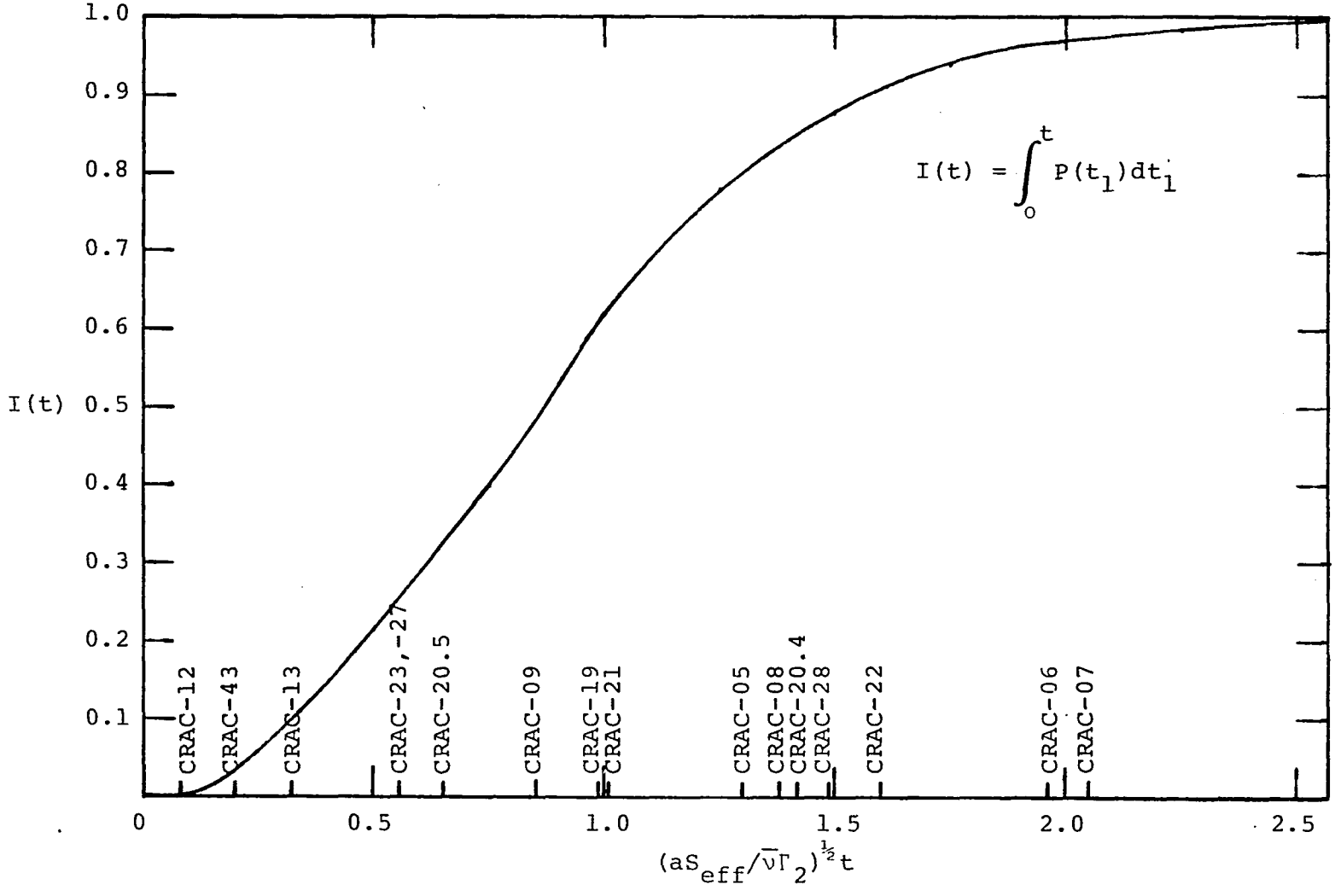

Figure 3.7. Integration of probability vs distribution of experiments.

case with seventeen of the twenty-nine experiments. Ten experiments did not involve prompt critical volumes of solution and hence do not meet the conditions of Hansen's analysis. Two experiments were not in the range of the plot and are discussed in Chapter 5. The histogram in Figure 3.8 provides another method for illustrating the results of Figure 3.7. Here the experimental results are superimposed on the theoretical curve which was generated using Eq. (2.26).

3.2 Nuclear Incident at the ICPP on January 25, 1961

On January 20, 1961, the ICPP (Idaho Chemical Processing Plant) began processing highly enriched uranium-aluminum fuels, after experiencing a lengthy shutdown. Initial extraction was of salvage material from previous runs. In addition to the startup of the extraction equipment, dissolution of ETR (Experimental Test Reactor) fuel was started on a planned 20-day run. This was the first "hot processing" using the equipment involved in the incident, in approximately 12 months. Two process cells, G and H, were routinely involved in dissolution and first cycle solvent extraction. A process flowsheet for H-Cell first cycle product wash is illustrated in Figure 3.9. The nuclear excursion occurred in the product evaporator (H-110) of the H-Cell first cycle product wash, and upon referring to

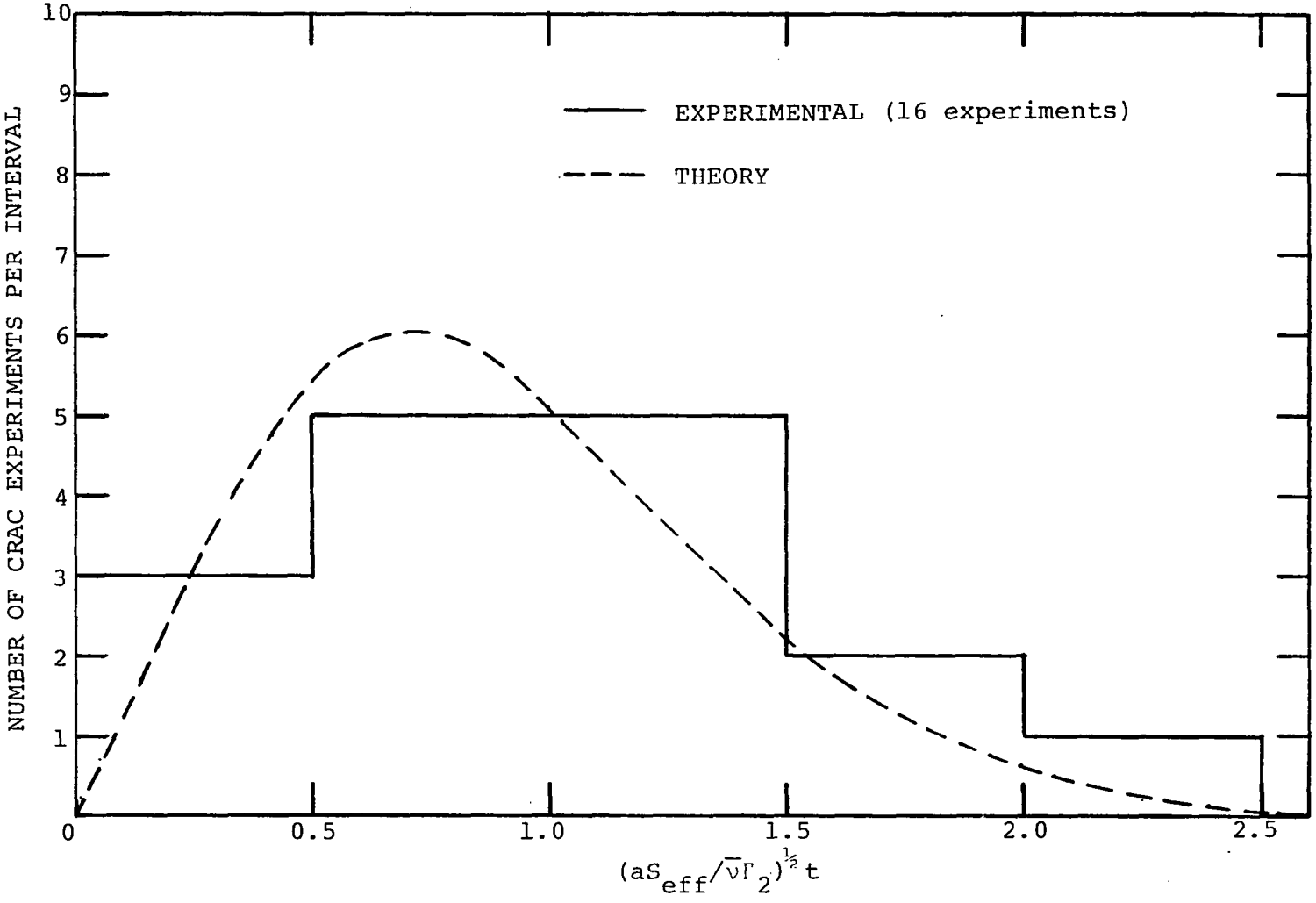

Figure 3.8. Number of CRAC experiments per interval vs distribution of experiments.

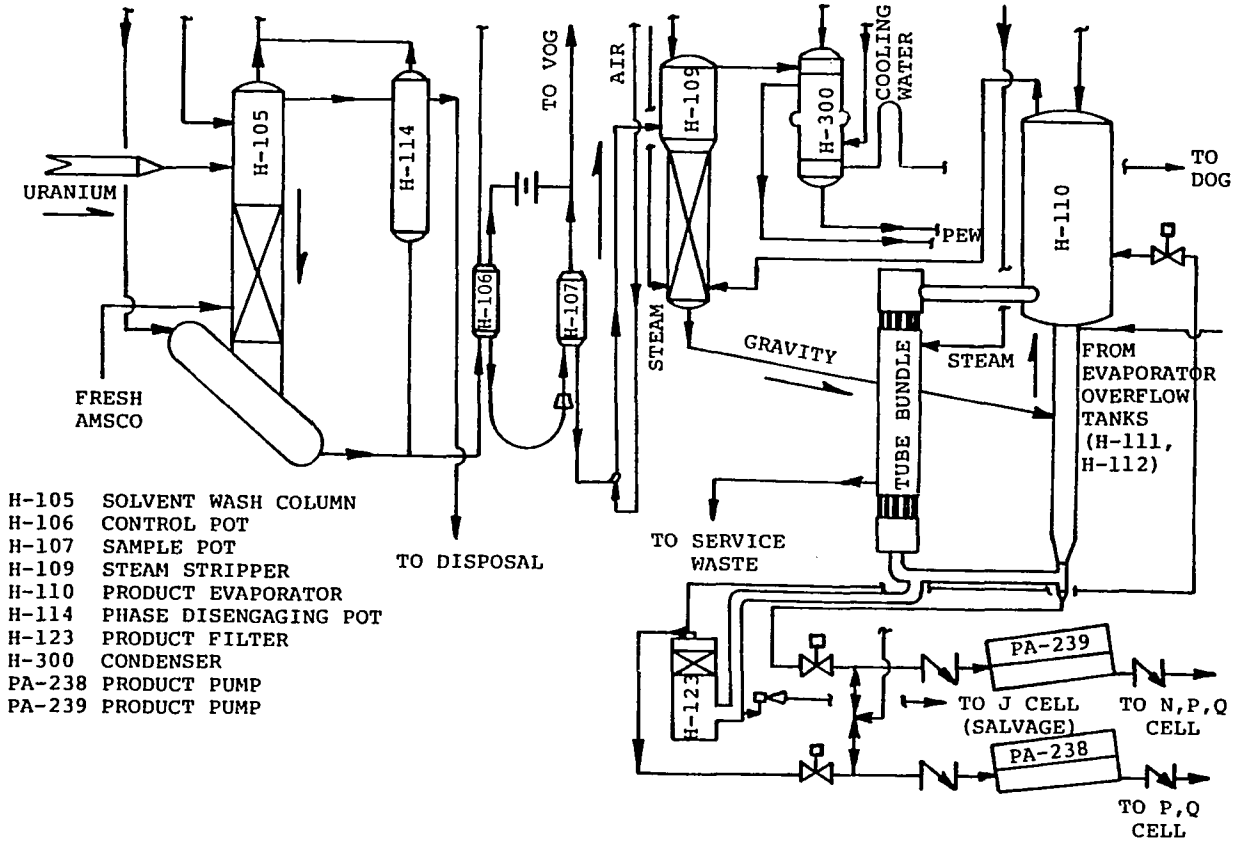

Figure 3.9. Process flowsheet for H-cell first cycle product wash.

Figure 3.9 the events leading to the excursion may be clearly traced.

The uranium shown entering from H-103 is contained in an aqueous solution recovered from the first cycle strip column. The normal evaporator feed concentration is four grams of uranium per liter; however, at the time of the incident the actual concentration was approximately 0.1 grams per liter. The uranium solution passes downward through the solvent wash column (H-105), in which it is contacted with fresh extraction solvent diluent. This packed column was designed to remove most of the dissolved tributyl phosphate extractant (TBP) from the aqueous uranium stream, thereby preventing its accumulation in the product evaporator with several undesirable effects. From the bottom of the column the aqueous uranium solution is air-lifted to the top of the steam stripper (H-109). Steam is admitted to the bottom of the packed section of the steam stripper and passes upward, stripping entrained or dissolved solvent diluent, as well as additional TBP, from the descending liquid before it reaches the evaporator. The overhead steam is condensed and routed to the process equipment waste (PEW) system for re-evaporation and disposal.

The aqueous solution flows by gravity from the steam stripper to approximately the mid-point of the cold leg of the product evaporator, where it is normally concentrated

about 50-fold, to 200 grams per liter. Since, at the time of the incident, the evaporator feed was very dilute, the concentration factor in the H-110 evaporator was on the order of 2000, resulting in a product concentration of 200 grams per liter. Because of the low evaporator product rate, intermittent rather than continuous pumpout had been scheduled. The evaporator product was normally transferred by a remote head diaphragm pump, PA-238 or PA-239 to either P-Cell or Q-Cell for second cycle extraction or by PA-239 to N-Cell for temporary storage, from which it may go to second cycle extraction.

The product evaporator is a continuous thermosiphon evaporator and feed to the evaporator mixes with material already concentrated. An application of heat to the tube bundle vaporizes part of the liquid in the tubes thereby discharging a mixture of liquid and vapor into the two-foot diameter vapor-disengaging space atop the cold leg. Steam from the top of the evaporator then flows to the bottom of the steam stripper and additional steam is introduced to give the desired vapor-liquid ratio. It was realized during design that the two-foot diameter vapor-disengaging space was not geometrically safe. As a safety measure, a 1½ inch diameter overflow line was provided below the two-foot diameter section. Overflow material is collected in two geometrically safe vessels (H-111 and H-112). Should these vessels fill,

additional material overflows to the cell floor rather than being allowed to back up into the critically unsafe expanded section of the evaporator.

Pumps PA-238 and PA-239 had never performed as desired. Considerable maintenance was required due to erratic pumping rates. On January 25, the specific gravity of the solution in the evaporator approached 1.28, indicating a uranium concentration of approximately 200 grams per liter and an attempt was made to pump material from H-110 to N-Cell. Pump PA-239 was started but failed to deliver. An attempt was made to clear the lines. This meant flushing the lines with water and air using the decontamination equipment. The discharge line was apparently cleared and the pump suction line from H-110 to PA-239 was air-purged. The pump still would not deliver. All attempts to start the pumpout of H-110 to N-Cell failed. During this time, the columns were on recycle feed and there was only a very slight build-up of uranium in the H-110 evaporator.

In order to prevent further dilution of the first cycle product in N-Cell by the water used for flushing and testing, pumping to J-Cell was attempted. Instrument response of transfers to J-Cell is quicker than N-Cell because of shorter piping runs. The discharge lines of both pumps to J-Cell were flushed with water. The suction lines were purged from the pumps back into the evaporator with steam.

Again, an attempt to pump through PA-239 failed. Flow was established through PA-238 for a short time, indicating that this pump was operating satisfactorily and the suction line from the evaporator was not plugged. Either the discharge line from PA-239 was plugged or that pump was not functioning properly. Since PA-238 discharge is not routed to N-Cell, further attempts were made to make PA-239 operate.

Immediately prior to the time of the incident, an operator in the process makeup area was instructed to put approximately four liters of water into the 10-gallon flushing tank and use 40 psig air pressure to move it into the decontamination line. The process operator at the control panel then opened the PA-239 discharge valve to J-Cell. A buildup of liquid in the J-Cell storage vessel equivalent to four liters was noted. The operator in the makeup area was then instructed to close the valve from the decontamination tank. A reply was noted, however the words were not distinguishable. Pump PA-239 was then started and momentarily ran with the suction valve from H-110 closed. The process operator had hardly taken his hand off the valve (PA-239 suction) control after opening the valve when radiation alarms sounded throughout the plant. A residuum from an earlier line unplugging operation using high pressure air forced about 40 liters of 200 grams per liter uranyl nitrate solution up a critically safe pipe into the critically unsafe

vapor-disengagement cylinder. The excursion occurred in a 356 liter cylindrical tank probably as a single power spike as the 40 liters were marginally sufficient to create a critical system in a vessel having a diameter of two-feet. The yield was estimated at 6×10^{17} fissions with an error not to exceed 25%, and no estimates were available for the reactivity and power history.

The details of this incident clearly illustrate an example of the "operational abnormalities" mentioned in Chapter 1. Using the theory presented in Chapter 2, it is of interest to determine whether this incident qualifies as a strong or weak source condition. This may be determined by evaluating the quantity $2S\tau/\bar{\nu}\Gamma_2$. The estimated concentration is 200 grams of uranium per liter, 90% enriched in U-235. Based on 93% enriched data the spontaneous fission and (α,n) neutron source strength, S, was calculated and is 620 neutrons per second. Leakage of neutrons was then taken into consideration using Eq. (3.1). From ARH-600 (Carter, Kiel, and Ridgway, 1969) and for 200 grams of uranium per liter it was found that $\lambda_{ext} = 2.05$ cm and $M^2 = 27$ cm^2 for 93.5% enriched uranyl nitrate solution. The critical height of the 40 liter solution was found to be 13.74 cm and using Eq. (3.3) the geometric buckling then becomes 3.65×10^{-2} cm^{-2}. The "effective" source strength, S_{eff}, is then 310 neutrons per second.

Figure 3.3, constructed from the CRAC experiments, yields 13.7 μ seconds as the mean neutron lifetime, τ, for a 93% enriched uranyl nitrate solution at 180 g U-235/liter. The quantities $\bar{\nu}$ and Γ_2 are for this incident 2.44 neutrons per fission and 0.8 respectively.

The condition of source strength, $2S_{eff}\tau/\bar{\nu}\Gamma_2$, then has a value of 4.4×10^{-3} and hence satisfies the weak source condition. Since this has the same magnitude as those calculated for the CRAC experiments, the curve illustrating the probability of the first persistent fission chain sponsored at time t_1, Figure 3.6, would be directly applicable. Recall that this figure represents an ensemble of CRAC experiments. Realizing this congruity and using the integrated probability curve illustrated in Figure 3.7, a range of the reactivity addition rate may be determined.

The CRAC experiment whose U-235 concentration corresponds the closest to 180 grams per liter is CRAC-43 which has a concentration equal to 188 grams U-235 per liter. The excursion occurred in a 610 mm diameter cylindrical tank, and CRAC-43 is an 800 mm diameter cylinder. This experiment has a total yield in the first pulse of 1.3×10^{17} fissions and a corresponding peak power equal to 5.6×10^{18} fissions per second. Using this data along with the volume in which the excursion occurred, a specific peak power may be calculated and is 1.4×10^{14} fissions/cm^3-sec. Figure 3.10 is a

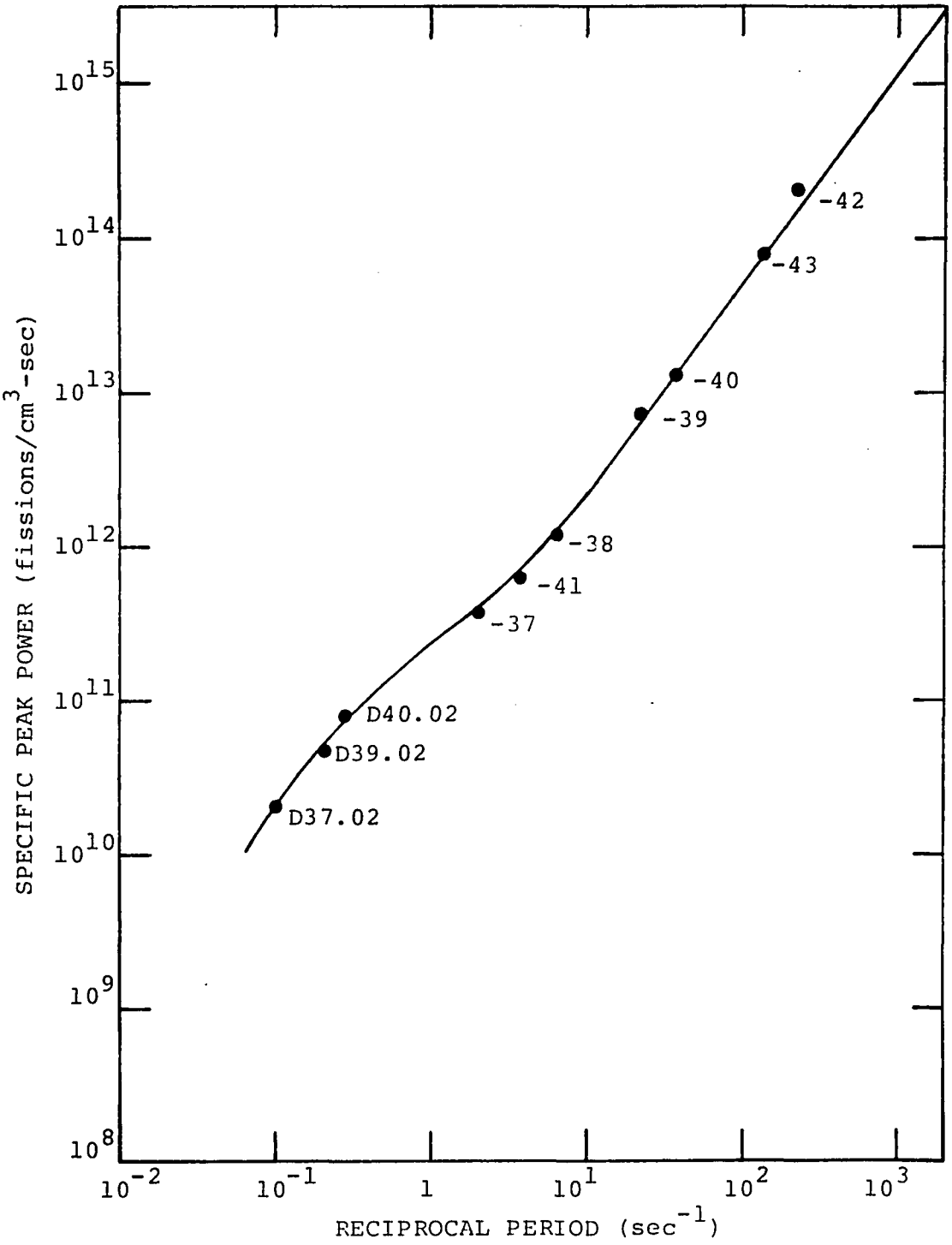

Figure 3.10. Specific power at peak of first pulse vs reciprocal period for the 800 mm dia cylinder.

curve taken from the report of the CRAC experiments and the reciprocal period, ω, may be determined from this curve knowing the specific peak power. For this incident the reciprocal period was found to be 199.53 sec^{-1}.

Assuming that the reactivity introduced in the single power spike was on the order of a dollar, it is convenient to work with the instantaneous reciprocal period; i.e.,

$$\omega = \frac{1}{n}\frac{dn}{dt} = \frac{\rho-\beta}{\tau} \tag{3.4}$$

where ρ = at and β = 0.00650. The quantity (at) may then be evaluated and used in determining a reactivity addition rate. Referring back to Figure 3.7, consider three values of I(t), namely 0.1, 0.5, 0.9 and the corresponding value on the abscissa, x_{abs}, such that:

$$\left(\frac{aS_{eff}}{\bar{\nu}\Gamma_2}\right)^{\frac{1}{2}} t = x_{abs} \tag{3.5}$$

Solving Eqs. (3.4) and (3.5) simultaneously, a reactivity addition rate may be calculated for each of the values of I(t). The results are listed in Table 3.6 with the addition rates in dollars per second using β_{eff} = 0.00825.

Table 3.6. Reactivity addition rate for the ICPP.

I(t)	$\left(\frac{aS_{eff}}{\bar{\nu}\Gamma_2}\right)^{\frac{1}{2}} t$	Time of Burst $t=t_1+t_2$ (sec)	Reactivity Addition Rate (dollars/sec)
0.1	0.32	0.07	16.062
0.5	0.85	0.49	2.276
0.9	1.56	1.66	0.676

In the next section, these results are noted on the appropriate integrated probability curve. Ramp rates greater than about 1.0 dollar/sec are likely excessive so that a relatively late burst seems likely. Nevertheless, the above range of ramp rates are physically achievable and generally consistent with the CRAC analysis.

3.3 Accidental Criticality at Wood River Junction, R.I. on July 24, 1964

This processing accident occurred in the United Nuclear Corporation's U-235 scrap recovery facility. The plant was designed to recover enriched uranium from unirradiated scrap resulting from the fabrication of reactor fuel elements. Because of start-up difficulties, an unusually large amount of uranium-contaminated trichloroethane (TCE) solution had accumulated. The low-concentration uranium in this solution is laboriously recovered by mixing and hand-agitating the TCE with sodium carbonate solution. Prior to

July 17, 1964 this operation was performed by hand in small 11 liter bottles of safe dimensions. On that date, because of the large amount of solution that had accumulated, the operation was shifted to a 104 liter sodium carbonate makeup tank. This tank is cylindrical in geometry and unsafe for concentrated solutions; however, only dilute solutions were expected in this operation.

The day before the accident a plant evaporator malfunctioned, and upon investigation a plug of uranium nitrate crystals was found in a connecting line. These crystals were dissolved with steam, and the resulting 238 grams U-235 per liter solution was drained into polyethylene bottles identical to those used to store the low concentration TCE. On July 24, an operator carrying an 11 liter bottle of this solution thought it was TCE and poured the 93% enriched uranyl nitrate solution into the makeup tank containing 41 liters of 0.54M sodium carbonate solution. The solution was being agitated by an electric stirrer; a critical configuration was achieved, and a burst occurred when nearly all the uranium had been transferred. This burst of approximately 1.1×10^{17} fissions created a flash of light splashing about one-fifth of the solution out of the makeup tank, and knocking the operator to the floor. He was able to regain his footing and run from the area to an emergency building some 200 yards distant, but his radiation dose, which was

estimated to be 10,000 rads, was fatal and he died 49 hours later. As indicated in Table 1.1 this was the second fatality from accidents involving supercriticality of solutions and there have been none since then. A second burst occurred 2 hours later due to an on-off stirring motion with a yield of approximately 2×10^{16} fissions. No estimates were available for the reactivity and power history.

It is of interest to again determine whether this incident qualifies as a strong or a weak source condition. The estimated concentration is 54 grams of uranium per liter, 93% enriched in U-235. Based on the foregoing information the spontaneous fission and (α,n) neutron source strength, S, was calculated and is 220 neutrons per second. Leakage of neutrons is again significant and an effective source strength, S_{eff}, may be calculated using Eq. (3.1). The critical height of the 52 liter uranyl nitrate solution is 31.7 cm; using Eq. (3.3) the geometric buckling becomes 1.71×10^{-2} cm^{-2}, having used 2.02 cm for the extrapolation distance. The thermal migration area was taken from ARH-600 and was found to be 28.6 cm^2. Based on these values the effective source strength becomes 148 neutrons per second. Figure 3.3 indicates 39.5 μseconds as the mean neutron lifetime for 93% enriched uranyl nitrate solution. The quantities $\bar{\nu}$ and Γ_2 for this incident are again 2.44 neutrons per fission and $\Gamma_2=0.8$.

The condition of source strength, $2S_{eff}\tau/\bar{\nu}\Gamma_2$, then has a value of 6.0×10^{-3} and therefore satisfies the weak source condition. Again, the interpretation of this quantity is as discussed in the CRAC experiments and is of the same magnitude as those calculated for the CRAC experiments. Therefore, Figure 3.6 is directly applicable to this incident, and Figure 3.7 may again be used to calculate a range of the reactivity addition rate.

The CRAC experiment whose U-235 concentration corresponds closest to 54 grams per liter is CRAC-03 which has a concentration equal to 48.6 grams U-235 per liter. The excursion occurred in a 457 mm diameter cylindrical tank, and CRAC-03 is a 300 mm diameter cylinder. This experiment has a total yield in the first pulse of 1.7×10^{17} fissions and a corresponding peak power equal to 4.7×10^{15} fissions per second. Using this data along with the volume in which the excursion occurred, the specific peak power is 9.04×10^{10} fissions/cm^3-sec. Figure 3.11 is a curve taken from the report of the CRAC experiments and the reciprocal period, ω, may be determined from this curve knowing the specific peak power. For this incident the reciprocal period was found to be 0.35 sec^{-1}.

Referring again to Figure 3.7, consider three values of I(t), namely 0.1, 0.5, 0.9 and the corresponding values on the abscissa, x_{abs}. Upon solving Eqs. (3.4) and (3.5)

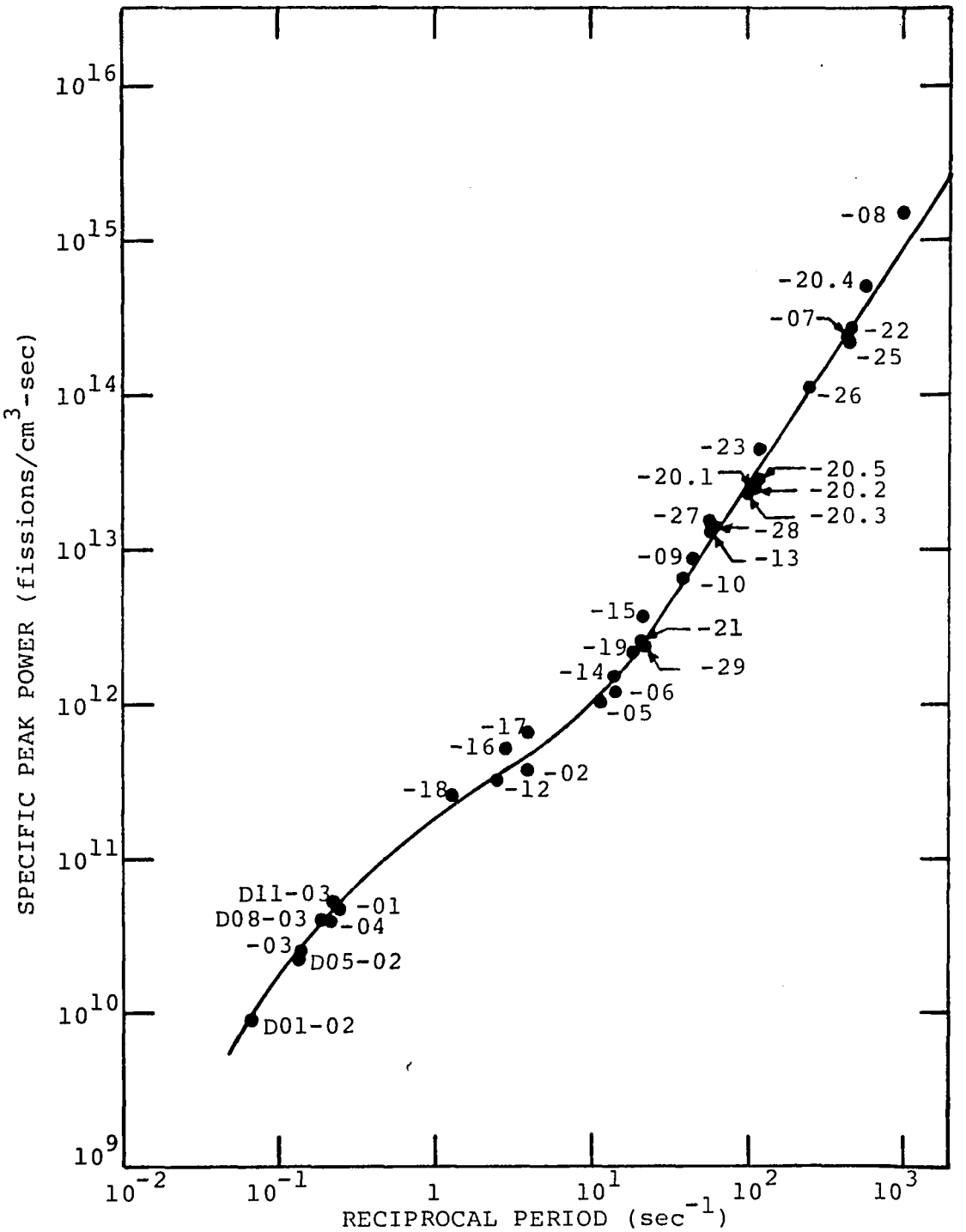

Figure 3.11. Specific power at peak of first pulse vs reciprocal period for the 300 mm dia cylinder.

simultaneously, a reactivity addition rate is calculated for each of the values of I(t). The results are listed in Table 3.7 with the addition rates in dollars per second using $\beta_{eff} = 0.00777$.

Table 3.7. Reactivity addition rates for WRJ.

I(t)	$\left(\frac{aS_{eff}}{\bar{\nu}\Gamma_2}\right)^{\frac{1}{2}} t$	Time of Burst $t=t_1+t_2$ (sec)	Reactivity Addition Rate (dollars/sec)
0.1	0.32	0.21	4.041
0.5	0.85	1.46	0.573
0.9	1.56	4.93	0.170

Figure 3.12 illustrates a range of the rate of reactivity for both the ICPP and WRJ using the same integrated probability curve as shown in Figure 3.7. They appear to be consistent with the CRAC analysis involving the assembly of fissionable material in the presence of a weak source, and indicate a range that is physically achievable.

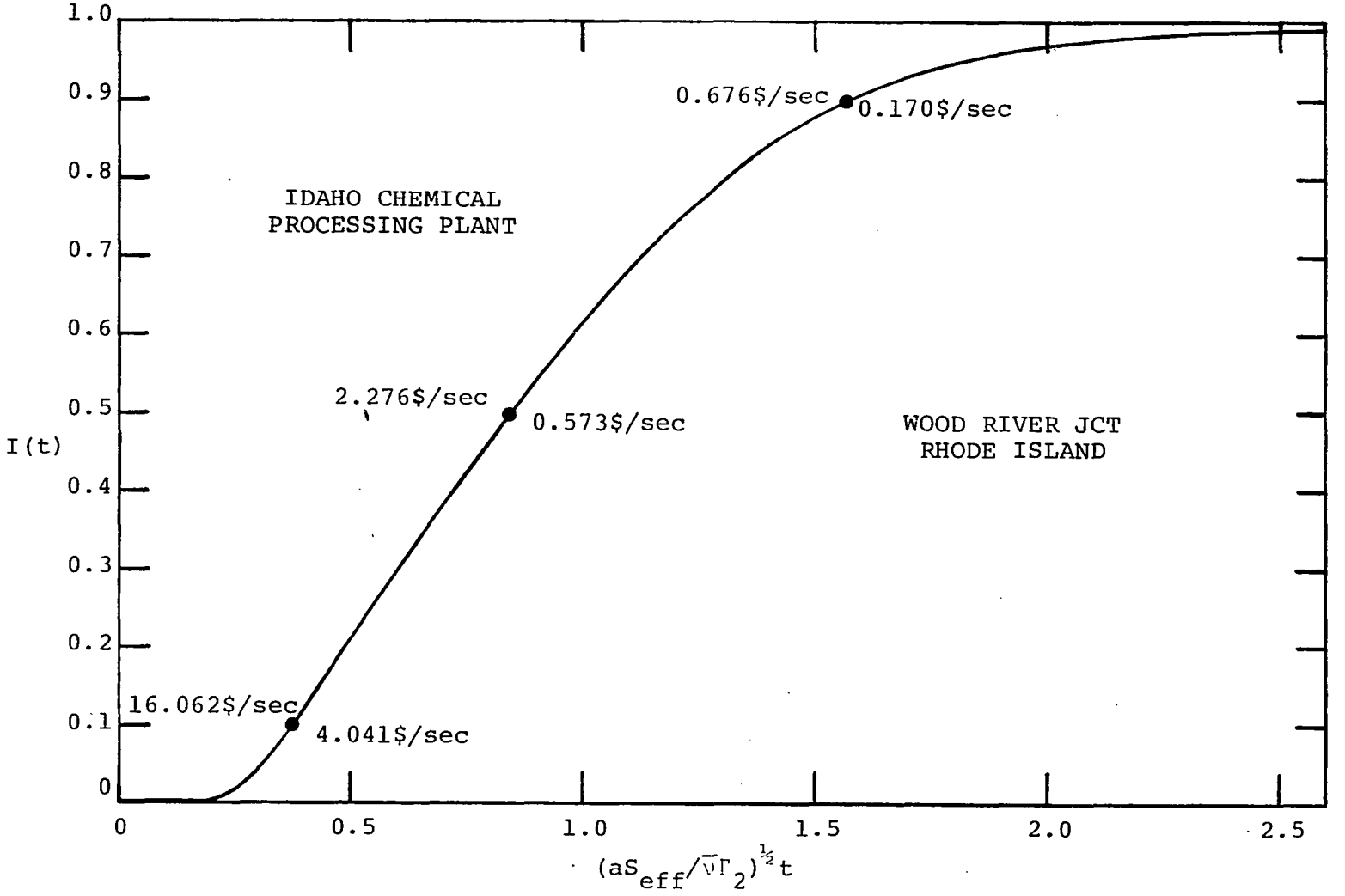

Figure 3.12. Integration of probability vs $(aS_{eff}/\bar{\nu}\Gamma_2)^{\frac{1}{2}}t$.

CHAPTER 4

THE AGNS DISSOLVER TANK

Fuel in commercial light-water reactors requires periodic removal and reprocessing because of (1) reactivity loss due to burnup and fission product production, (2) fuel integrity loss due to irradiation damage and/or corrosion, and (3) any other damage sustained by fuel bundles during their thrice-burn depletion period. Reprocessing entails three separate phases: (1) the mechanical separation of the fuel material from the cladding and assembly structural material, (2) the chemical separation of the unused uranium and produced plutonium, and (3) the separation of the uranium and plutonium for refabrication or storage.

As a first step in light-water reactor fuel reprocessing, Allied General Nuclear Services (AGNS) proposes to chop the fuel assemblies into pieces ranging from six to nine inches in length depending on the dissolution of the dissolver, and discharge the pieces into a large cylindrical dissolver tank. The dissolver tank is a chemical reaction vessel containing a large volume of solution composed mainly of nitric acid and water. The nitric acid reacts with the uranium dioxide to form uranyl nitrate, nitrogen dioxide,

and water with the accompanying evolution of heat. The nitric acid does not dissolve the cladding or the structural material. The dissolver tank has an internal basket with which the undissolved material may be removed at periodic intervals.

The dimensions of the dissolver tank, ∿80 cm in diameter and ∿485 cm in height, are such that criticality is possible when filled with the standard 1000 liter dissolver load of solution to a height of 205 cm. However, the design of the dissolver incorporates a normal solution density control of 1.49 grams of solution per cubic centimeter which corresponds to a U-235 concentration of 14.7 grams per liter. Actual criticality of this solution alone is not possible, but when chopped segments of light-water reactor fuel are added to the solution, the system can become critical to an extent that depends on fuel enrichment, burnup, the concentration of the dissolved poison (gadolinium), and obviously the amount of chopped fuel added. Thus, the operation of the dissolver is based on the presence of gadolinium as a distributed poison in the solution and limited batch sizes for fuel added to the tank.

As the dissolver operates, the layer of dissolved uranium dioxide developing in the solution is decanted at a rate such that the solution density does not exceed the limit

of 1.55 grams of solution per cubic centimeter. This corresponds to a U-235 concentration of 15 grams per liter.

Recognizing the potential for criticality, the following question was raised: Should a batch error occur, would enough reactivity exist such that the system would reach prompt critical and cause a large fission burst? In order to provide an answer to this question an analysis using the theory discussed in Chapter 2 is in order. The solution is considered to be a homogeneous mixture of uranium enriched to 5 wt.% U-235, water, and nitric acid.

In order to obtain an upper bound on this analysis, it will be assumed that there are no poisons present in the dissolver.

Of particular interest is whether this system constitutes a strong or a weak source condition. This may be determined by evaluating the quantity $2S\tau/\overline{\nu}\Gamma_2$. It will be assumed that the source strength, S, is due to spontaneous fission and (α,n) reactions on oxygen in the dissolver solution.

In calculating the source contribution due to the amount of chopped fuel added, data from the Yankee Rowe Reactor supplied by AGNS will be used. This data is listed in Table 4.1 with the initial enrichment being 5.00 wt.% U-235, and an exposure of 5000 MWD/MTM; i.e., the fuel is virtually unirradiated. The fissile material inventory was

Table 4.1. Isotopic composition of Yankee Rowe Reactor fuel.

Composition	wt.% of Fuel
Uranium	87.40
Plutonium	0.23
Fission Products	0.52
Oxygen	11.85
U-235	4.45
U-236	0.174
U-238	95.38
Pu-238	0.18
Pu-239	92.16
Pu-240	5.80
Pu-241	1.77
Pu-242	0.09

determined using a fuel assembly length of 9 feet 3½ inches, with 204 fuel pins containing 412,600 grams UO_2 per assembly. This quantity and the data in Table 4.1 yield the material inventories listed in Table 4.2. Knowing the inventories for the various isotopes of uranium and plutonium, and using the neutron emission rates for these isotopes which are listed in Table 4.3, the spontaneous fission source strength was determined. The neutron emission rates listed in Table 4.3 were taken from Johnson and Ombrellaro (1981). This then gives the source contribution due to the addition of the fuel assembly, and is equal to 58,200 neutrons per second. The source contribution due to (α,n) reactions on oxygen was determined using ANSOURCE (Appendix B) and was found to be 114,600 neutrons per second, yielding a total source strength, S, equal to 172,800 neutrons per second. Since this source term is so large, leakage of neutrons is significant. Using ARH-600 (Carter et al., 1969) it was found that $M^2 = 33\ cm^2$, and $\lambda_{ext} = 2.53$ cm for a 5% $UO_2(NO_3)_2$ solution, 315 grams of uranium per liter. Using Eq. (3.3) the geometric buckling becomes $3.42 \times 10^{-3}\ cm^{-2}$, and hence using Eq. (3.1) the "effective" source strength, S_{eff}, is 155,300 neutrons per second.

In nitrate solutions the neutron lifetime, τ, varies strongly with U-235 concentration. Should a criticality accident occur, it will be assumed that the U-235

Table 4.2. Fuel assembly fissile material inventory.

Composition	Mass of Fuel (grams)
Uranium	360,605
Plutonium	949
Fission Products	2,145
Oxygen	48,892
U-235	16,047
U-236	627
U-238	343,945
Pu-238	1.7
Pu-239	875
Pu-240	55
Pu-241	16.8
Pu-242	0.8

Table 4.3. Spontaneous neutron emission rates for uranium and plutonium isotopes.

Isotope	Spontaneous Fission Yields (neutrons/gm-sec)	SF Source Strength (neutrons/sec)
U-235	2.727×10^{-4}	4.4
U-236	4.998×10^{-3}	3.1
U-238	1.079×10^{-2}	3,711
Pu-238	2.197×10^{3}	3,753
Pu-239	2.082×10^{-2}	18.2
Pu-240	8.950×10^{2}	49,260
Pu-241	4.939×10^{-2}	0.8
Pu-242	1.716×10^{3}	1,466
	TOTAL	58,216

concentration would increase to approximately 100 grams per liter. This corresponds to a neutron lifetime of 2.5×10^{-5} seconds. The quantities $\bar{\nu}$ and Γ_2 are 2.30 neutrons per fission and 0.8 respectively.

The condition of source strength, $2S_{eff}\tau/\bar{\nu}\Gamma_2$, then has a value of 4.2 and hence clearly qualifies as a strong source. This quantity represents the "expected" number of persistent fission chains being sponsored in the interval $0 \leqslant t \leqslant t_1$. It is during this interval that reactivity is applied to the system in the form of chopped pieces of fuel being added to the dissolver solution. A reactivity addition rate may be determined by assuming that 6-inch segments of fuel are being added to the solution. The mass of fuel added in each chopping operation contributes to the inventory of the dissolver; its reactivity worth is estimated to be given by

$$\rho^+ = m_{fc} \frac{\Delta\rho}{\Delta m} \tag{4.1}$$

where

ρ^+ is the reactivity added

m_{fc} is the mass of fissile material added in a single chop

$\Delta\rho/\rho m$ is the reactivity added per unit mass of fissile material added

It was found that there are 412,600 grams UO_2 in one complete fuel assembly. Therefore, for a 6-inch chop there are 22,250 grams UO_2. Using the information supplied in Table 4.1 for the isotopes of U-235, Pu-239, and Pu-241 the value of m_{fc} = 0.9135 kg of fissile material. For the PWR fuel considered, the largest value of $\Delta\rho/\Delta m$ is 0.133 \$/Kgm (Verdon, 1975). The value of ρ^+, the reactivity added in one 6-inch chop, is then equal to 0.1215 dollars. The rate of addition is dependent on the rate at which the 204 pieces from each segment are transferred to the dissolver solution. If all the pieces enter more or less simultaneously, the reactivity addition is in the form of a "step" change. If the pieces "dribble" in, a "ramp" addition is realized. It will be assumed that the addition is a ramp rate, and that the interval between chops is between ten and twenty seconds. The average reactivity addition rate is then equal to 0.00877 dollars per second. Using a value of β_{eff} = 0.0070 this then becomes 6.142×10^{-5} sec^{-1}.

Knowing the rate of reactivity addition, and using Eq. (2.25c), the probability of the first persistent fission chain being sponsored at time t_1 may be determined. Figure 4.1 illustrates this probability, and it is seen that persistent fission chains sponsored prior to the system reaching critical play a significant role in determining the average time for the neutron population to reach a prescribed value.

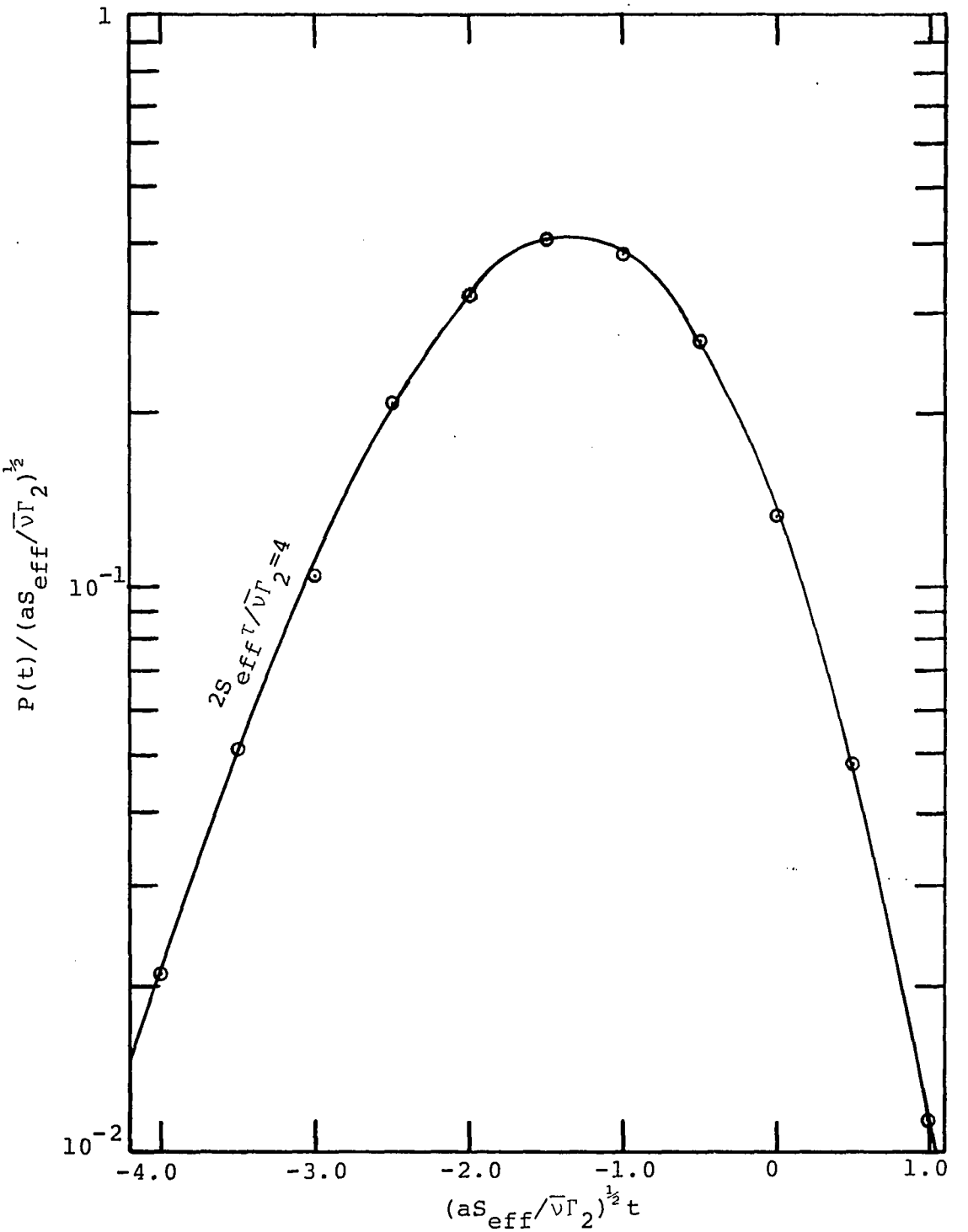

Figure 4.1. Probability of the first persistent fission chain under a ramp insertion.

Should a batch error occur, in order for this system to go prompt critical, which would involve the failure of the double contingency principle, the total reactivity would be equivalent to one dollar and therefore for a ramp reactivity increase, ρ = 1.00\$ = at. Using the value previously determined for a, the time needed to go prompt critical is 114 seconds or approximately 1.9 minutes. It is of interest to determine at this point the probability of this system reaching prompt critical, and this may be done using Hansen's theory.

When a strong source condition exists, it is not necessary to treat k_{eff} as a time-dependent quantity as is the case with a weak source condition. There is no delay between the time of criticality and the time of the first persistent fission chain as there is in a weak source case. Fluctuations in time occur in a weak source case whereas for the strong source case this is not necessarily true, depending on the magnitude of $2S\tau/\bar{\nu}\Gamma_2$. Using Eq. (2.7) we have the probability of a source neutron sponsoring a persistent fission chain equal to 9.24×10^{-4} and therefore the expected number of persistent chain initiations per second is $W \cdot S$ = 144. The average time between successive initiations is $1/W \cdot S$ and is equal to 0.0070 seconds. The magnitude of this number indicates that the system will never go prompt critical. The probability of the first persistent fission chain

between the time of $k_{eff} = 0$ and a time t' following $k_{eff} = 0$ is

$$P(0,t') = WS \int_0^{t'} e^{-WSt}\, dt \qquad (4.2)$$

Solving Eq. (4.2) for 1 second yields $P(0,t') = 1.0$. Solving Eq. (4.2) for 1 millisecond yields $P(0,t') = 0.134$ and hence the probability of the first persistent fission chain after $\rho=\beta$ is given by

$$P(t_p,\infty) = WS \int_{t_p}^{\infty} e^{-WSt}\, dt \qquad (4.3)$$

where t_p is the time at which $\rho=\beta$ and upon attempting to solve Eq. (4.3), for all purposes $P(t_p,\infty)=0.0$ and hence this system will never go prompt critical. The dissolver solution will go delayed critical well before prompt criticality can be achieved. Hence a large burst will not be expected.

CHAPTER 5

CONCLUSIONS AND SUMMARY

The intent of this study was to examine the influence of reactivity addition rate and source strength on the critical behavior of low and highly enriched uranyl nitrate solutions. In doing this, Hansen's paper (1960) was validated by performing a modified one-group calculation on systems of 5% and 93% enriched uranium.

Chapter 1 presented a brief introduction of nuclear criticality safety and enlightened the reader as to the types of criticality accidents that have occurred in the past years. In Chapter 2, the theory presented in Hansen's paper was outlined with the equations derived in detail. This then set the stage for testing the validity of this theory as applied to cylindrical systems.

Chapter 3 addressed the CRAC experiments and two criticality incidents presented in Table 1.1. Some of the CRAC experiments that were performed without an external source present showed significant delays in the initiation of a fission burst. This study focuses on these experiments as to the likelihood of obtaining a large destructive burst.

These experiments consisted of a wide range of uranium concentrations and ramp rates as solution was

injected into these tall narrow cylinders beyond the volume sufficient for criticality and was allowed recriticality. Of the 29 experiments considered, 17 experienced a fission burst at approximately the same time regardless of ramp rate and source strength. Ten experiments did not achieve prompt critical since criticality was under the influence of delayed neutrons, and two experiment time measurements malfunctioned. Out of the 29 experiments considered, only the experiments that had a dollar's worth of reactivity added at the peak of the first pulse are of interest, since Hansen's analysis does not take into consideration the effects of delayed neutrons. There were twenty of these experiments; all others were neglected.

The report on the CRAC experiments indicate that for the experiments assembled without an external source present, standard neutron kinetics is obeyed for low ramp rates. However, as the ramp rate increases above 0.05 dollars per second and approaches one dollar per second, these experiments show an increasing tendency for significant delays in the initiation of a pulse and hence result in larger pulse peaks; i.e., these experiments diverge from the standard kinetics family.

This study provides the basis for what constitutes a delayed burst. It was found that the CRAC experiments satisfied the weak source condition, and that they include

both standard kinetics behavior as well as show tendencies of a delayed burst. The basis for this difference is source strength and ramp rate. With a weak source condition reactivity may be added for a long time before the system is disturbed in the form of a power increase. In the case of experiments 7, 8 and 25 where the ramp rates are approaching one dollar per second, these pulses have peak yields 20-100 times that predicted by standard kinetics. However, it was shown that even though these experiments did go prompt critical they experienced a burst at about the same time as those governed by standard kinetics, and hence there was no significant delay in the initiation of the burst.

The analysis involving the two criticality incidents of Table 1.1 resulted in an average ramp rate in a range that is physically achievable and generally consistent with the KEWB experimental results for sulfate solutions.

Finally, Chapter 4 considered a system of low enrichment which satisfied the strong source condition. Here it was assumed that a complete fuel assembly was added to a dissolver tank with a total loss of soluble poison. It was found that it would take approximately two minutes from the addition of the complete fuel assembly to reach prompt critical. This would involve the failure of the double contingency principle so it is a remote accident scenario. However, based on the low ramp rate involved, if a batch error was to occur, the probability of obtaining a large

burst criticality accident is extremely small. A fission chain would be initiated in the dissolver shortly after criticality is reached and well before enough additional reactivity to make the solution prompt critical; hence there would be no large burst.

APPENDIX A

REACTIVITY ANALYSIS

It is of interest to determine how the reactivity changes with height as solution is injected into the 300 mm and 800 mm diameter cylinders at a constant rate. This may be illustrated using one-group theory, in order to arrive at an equation for reactivity as a function of height.

The effective multiplication factor is the product of the nonleakage probability, P_{NL}, and the infinite multiplication factor, k_∞. The following equation may be written:

$$k_{eff} = \frac{k_\infty}{1 + M_T^2 B^2} \tag{A.1}$$

From the basic definition of reactivity, the following equation may be obtained:

$$\rho = \frac{k - \left(1 + M_T^2 B^2\right)}{k_\infty} \tag{A.2}$$

and upon further simplification, a more useful form may be obtained:

$$\rho = 1 - \frac{1}{k_\infty} - \frac{M_T^2}{k_\infty} B^2 \tag{A.3}$$

which has the form $\rho = a - bB^2$. For a cylinder of radius R and height H,

$$B^2 = \left(\frac{2.405}{R}\right)^2 + \left(\frac{\pi}{H}\right)^2 \qquad (A.4)$$

and upon adding solution to a constant radius cylindrical tank, the following equation is obtained:

$$\rho = 1 - \frac{1}{k_\infty} - \frac{M_T^2}{k_\infty}\left(\frac{2.405}{R}\right)^2 - \frac{M_T^2}{k_\infty}\left(\frac{\pi}{H}\right)^2 \qquad (A.5)$$

Let

$$c = 1 - \frac{1}{k_\infty} - \frac{M_T^2}{k_\infty}\left(\frac{2.405}{R}\right)^2 \quad \text{and} \quad d = \frac{\pi^2 M_T^2}{k_\infty} \; .$$

Reactivity then has the following form and is a function of height:

$$\rho = c - \frac{d}{H^2} \qquad (A.6)$$

Taking the first derivative with respect to H yields:

$$\frac{d\rho}{dH} = \frac{2d}{H^3} = \frac{2\pi^2 M_T^2}{k_\infty H^3} \qquad (A.7)$$

and this equation determines the reactivity change per fractional change in height. At criticality $\rho = 0$, and $c = d/H_c^2$; using this boundary condition and Eq. (A.6), Figures 3.4

and 3.5 were generated. In order to obtain the reactivity increase from criticality to a particular height of the solution, Eq. (A.7) was integrated from H_c to H_x, and the following equation results:

$$\rho_x = - \frac{\pi^2 M_T^2}{k_\infty} \left(\frac{1}{H_x^2} - \frac{1}{H_c^2} \right) \tag{A.8}$$

It was found, using data from CRAC-38, that the agreement between actual measurements and theory, differed by about 19%. Values of reactivity change obtained from theory were lower than values determined from actual measurements. For example: if reactivity as a function of height is fairly linear between H_c and H_f, then the ramp rate may be defined as

$$a \equiv \frac{d\rho}{dt} = \frac{d\rho}{dH} \cdot \frac{dH}{dt} \tag{A.9}$$

Let $\alpha = dH/dt$, which is a constant for all experiments. One may then solve for $\Delta\rho_a$, which should equal ρ_{cf} (cf means curve fit), the reactivity change in going from H_c to H_{cf}, as illustrated in Figure 3.5. From Eq. (A.9) one may then write:

$$\Delta\rho_a = \frac{a \cdot \Delta H_a}{\alpha} \tag{A.10}$$

Using data from CRAC-38 and Eq. (A.8), it was found that $\rho_{cf} = 0.821 \times 10^{-3}$. Then, using Eq. (A.10) $\Delta\rho_a = 1.024 \times 10^{-3}$,

thus indicating an 18.7% difference between the two quantities. Moreover, $a_{cf} < a$ when in fact a_{cf} should have been greater, making inaccurate any attempts to correct for the ramp rate above criticality. The ramp rate at H_c is 0.00368 dollars/sec; a_{cf} was calculated, using Eq. (A.9), as 0.00267 dollars/sec.

APPENDIX B

COMPUTER PROGRAMS

Many of the calculations performed in this thesis required simply a hand calculator. However, there were some calculations that required the use of a computer due to either the complexity of the equation, or a lengthy iteration was necessary.

The development of three programs were needed to complete the analysis of this thesis; i.e., ANSOURCE, CRAC, and AGNS. Each program is written in Fortran IV and may be executed on any computer, regardless of the job control language used. At this point it is necessary to present a brief description of each program.

ANSOURCE is a program utilized to calculate a neutron source strength due to (α,n) reactions with oxygen. The nuclear reactions involved are:

$$ {}_2\alpha^4 + {}_8O^{17} \longrightarrow {}_{10}Ne^{20} + {}_0n^1 \qquad (B.1) $$

$$ {}_2\alpha^4 + {}_8O^{18} \longrightarrow {}_{10}Ne^{21} + {}_0n^1 \qquad (B.2) $$

In a uranyl nitrate solution, four isotopes of uranium will be considered: U-234, U-235, U-236, and U-238. The U-234 isotope is the predominant contributor of alpha particles in

the above reactions, for low and high enrichment solutions. Even in low enrichment solutions the fraction of U-234 would have to be less than 0.032% in order for the U-235 isotope to become a more significant source of neutrons in (α,n) reactions.

The program ANSOURCE was developed using a general analysis presented in Johnson and Ombrellaro (1981), and it is instructive to briefly outline a portion of that analysis that pertains to the development of ANSOURCE.

The average number of neutrons per alpha decay may be defined as

$$\bar{\nu}_i(\alpha,n) = \sum_j f_{ij} P(E_{\alpha_{ij}}) \qquad (B.3)$$

where f_{ij}, the branching ratio, is the fraction of all alpha particles, j, with energies $E_{\alpha_{ij}}$ emitted by nuclide i and the values for these, for each isotope, were obtained from Browne, Dairiki, and Doebler (1978). $P(E_{\alpha_{ij}})$ is the probability of an (α,n) reaction occurring in the solution per alpha decay of nuclide i with an initial energy $E_{\alpha_{ij}}$. The sum is over each alpha decay branch, j, possible in nuclide i. Thus the term $P(E_{\alpha_{ij}})$ of Eq. (B.3) is the probability of the alpha particle emitted by a heavy metal isotope i to induce, as it slows down in the solution, an (α,n) reaction with either of the isotopes O^{17} or O^{18}. The higher the alpha-particle energy, the greater the probability that the (α,n) reaction occurs as the particle

slows down. The probability $P(E_\alpha)$ is calculated for each of the $^{17}O(\alpha,n)Ne^{20}$ and $^{18}O(\alpha,n)Ne^{21}$ reactions using the thick target yield expression

$$P(E_\alpha) = 10^{-30} \frac{\rho_T N_A}{\rho_S A_T} \int_0^{E_\alpha} \frac{\sigma_{\alpha,n}(E)\,dE}{(dE/d\rho X)} \qquad (B.4)$$

where for the $^{17}O(\alpha,n)Ne^{20}$ reaction, for example,

$\sigma_{\alpha,n}(E)\,dE$ = experimentally measured $^{17}O(\alpha,n)Ne^{20}$ reaction cross section in mb.

$(dE/d\rho X)$ = the stopping power as a function of energy for alpha particles slowing down in the solution, MeV/mg-cm^{-2}.

ρ_T/ρ_S = the ratio of the density of the O^{17} target in the solution to the total solution density.

A_T = atomic mass of O^{17} in amu.

N_A = Avogadro's number (6.02308×10^{23} atoms/mole).

E_α = initial energy of the alpha particle in MeV.

The same expression with appropriate changes is used to calculate the probability for the $^{18}O(\alpha,n)Ne^{21}$ reaction. The measured reaction cross sections were obtained from Johnson

and Ombrellaro (1981), who in turn obtained the data from the Oak Ridge National Laboratory. These data are given in Bair and Haas (1973), Bair and Willard (1962) and Bair and Gomez del Campo (1979). The first two references provide these target cross-section data for $^{17}O(\alpha,n)Ne^{20}$ and $^{18}O(\alpha,n)Ne^{21}$ reaction alpha-particle energies ranging from 1.3 to 5.15 MeV. However, the third reference shows that the cross sections of Bair and Haas (1973) and Bair and Willard (1962) should be multiplied by 1.35 in order to obtain calculated thick target yield data comparable to measured yields.

The stopping power dE/dX or dE/dρX given in Eq. (B.4) represents the energy loss by an alpha particle per unit path length. Ziegler and Chu (1974) show that the stopping power is proportional to the stopping cross section, and is given as

$$\frac{dE}{d\rho X} = \frac{N_A}{A} \varepsilon_\alpha \cdot 10^{-24} \qquad (B.5)$$

where ε_α is the stopping cross section for He^4 ions in some material. This cross section is generally given in units of electronvolts per 10^{15} atoms per cm^2. In this expression, ρ is the density in g/cm^3, A is the mass number of the material and N_A is Avogadro's number. In this form the units of $dE/d\rho X$ are chosen as MeV per $mg \cdot cm^{-2}$.

The stopping cross sections for the various nuclides were calculated using the fitting formulas and constants of Zeigler (1977). Since stopping powers of alpha particles in plutonium are not available in the literature, the stopping cross sections for plutonium were assumed to be equal to those of uranium for the use of ANSOURCE in Chapter 4. In calculating the probability $P(E_\alpha)$, the stopping powers were calculated using Eq. (B.5) and stopping cross sections were obtained from the fitting formulas of Zeigler (1977).

Upon using these equations one may now determine the total neutron source strength due to (α,n) reactions. $\lambda_i N_i f_{ij}$ is the number of alpha particles per cm^3 per second for each alpha particle energy. Hence the total neutron source strength due to (α,n) reactions is

$$S(\alpha,n) = V \sum_i \sum_j f_{ij} P(E_{\alpha_{ij}}) \lambda_i(\alpha) N_i \qquad (B.6)$$

where V is the volume in cm^3 of the system being considered. In order to use ANSOURCE for a system indicated on the listing shown in Figure B.1, one merely has to determine the number densities for each constituent in the system. The equation for solution density was provided by Forehand (1981) and the isotopic weights by Dyer (1981).

CRAC is a program utilized to calculate the probability distribution of the first persistent fission chain sponsored at a time t_1 in the interval dt_1. It is a small program, designed to solve Eq. (2.26)

$$P(t_1)dt_1 \cong \frac{2aS_{eff}t_1}{\bar{\nu}\Gamma_2} e^{-aS_{eff}t_1^2/\bar{\nu}\Gamma_2} dt_1 \qquad (B.7)$$

for all twenty-nine CRAC experiments, and is only useful for $t_1 \geq 0$. The listing for this program is shown in Figure B.2.

AGNS is a program also utilized to calculate the probability of the first persistent fission chain sponsored at a time t_1 in the interval dt_1. However, this program solves Eq. (2.25c)

$$P(t_1)dt_1 = \sqrt{\frac{2a\tau S^2}{\pi\bar{\nu}^2\Gamma_2^2}} \left[\frac{1-\text{erf}\left(\sqrt{\frac{a}{2\tau}}\, t_1\right)}{2}\right]^{\frac{2S\tau}{\bar{\nu}\Gamma_2}-1} e^{-at_1^2/2\tau} dt_1 \qquad (B.8)$$

for the large AGNS dissolver tank in Chapter 4. It is a program requiring no core memory, and executes in double precision. The listing for this program is shown in Figure B.3. Unlike the CRAC program, this is useful for all values of time, i.e., $-\infty < t_1 < \infty$.

Each of these two programs were written in double precision for reasons of interchangeability between the two. AGNS required an evaluation of the error function with

arguments as high as 3.00 and hence double precision was necessary. The ERF subroutine can evaluate arguments as high as 7.50 with an accuracy of 10^{-26}. This subroutine used the following series expansion:

$$\mathrm{erf}(z) = \frac{2}{\sqrt{\pi}} e^{-z^2} \sum_{n=0}^{\infty} \frac{2^n}{1 \cdot 3 \cdot 5 \ldots (2n+1)} z^{2n+1} \qquad \text{(B.9)}$$

along with a recursion relation, in order to evaluate the error function in Eq. (2.25c).

```
C     ************************************************************
C     ********************  ANSOURCE  ********************************
C     ************************************************************
C     THIS PROGRAM COMPUTES THE NEUTRON SOURCE STRENGTH FROM
C     (ALPHA,N) REACTIONS WITH OXYGEN 17 AND 18 DUE TO ALPHA
C     PARTICLES EMITTED FROM URANIUM DIOXIDE AND/OR PLUTONIUM
C     DIOXIDE AND NITRATE SOLUTIONS
C     ************************************************************
C     ************************************************************
C     *******                                        ***************
C     ********AUTHORS:                               ***************
C     *******           DR. ROBERT E. MILES          ***************
C     *******           GERALD B. DULCO              ***************
C     *******                                        ***************
C     *******DATE:      APRIL, 1982                  ***************
C     ************************************************************
      IMPLICIT REAL*8 (A-H,L-Z)
      COMMON /MSP/ N(13),P(13),A1(13),PF,AAVG,BAVG,ITYPE
      DIMENSION S(9),SUM1(9),SUM2(9),LAMBDA(12),TIT(12),
          TITLE(18),A(13),
     *ALPHAE(80),YF(80),S1(80),S2(80),P1(80),P2(80),E(750),
          E17(750),
     *E18(750),DE17(750),DE18(750),AN17(750),AN18(750),
          EAH(750),
     *EAN(750),EA0(750),EAU(750),EAP(750),EAH1(750),EAN1
          (750),EA01(750),
     *EAU1(750),EAP1(750),DEPX(750),DEPX1(750),DEX(750),
          DEX1(750)

      READ(5,35) (E17(I),DE17(I),AN17(I),I=1,748)
      READ(5,35) (E18(I),DE18(I),AN18(I),I=1,732)
      DATA A/1.007979,14.006763,15.999384,234.040947,235.
          043925,
     *236.045563,238.050786,238.049555,239.052158,240.
          053809,241.056847,
     *242.058739,0.602308/
      DATA LAMBDA/3*0.0,8.98E-14,3.0935E-17,9.1518E-16,
          4.9137E-18,
     *2.5030E-10,9.0055E-13,3.3600E-12,3.6359E-14,5.6755E-14/
      DATA ALPHAE/4.7744,4.7229,4.6026,4.598,4.557,4.503,
          4.446,4.416,
     *4.397,4.367,4.345,4.324,4.267,4.217,4.158,4.4943,
          4.4455,4.3318,
     *4.1964,4.1495,5.498,5.454,5.359,5.215,5.161,5.149,
          5.111,5.082,
     *5.070,5.060,5.035,5.014,5.005,4.992,4.967,4.961,4.941,
          4.918,
```

Figure B.1. List of ANSOURCE.

```
     *4.877,4.834,4.805,4.743,4.699,4.640,5.1589,5.115,
          5.014,4.851,
     *4.48,5.051,5.041,4.995,4.971,4.8959,4.8529,4.798,
          4.73,4.9009,
     *4.8566,1.0,1.25,1.50,1.75,2.0,2.25,2.50,2.75,3.0,3.25,
     *3.50,3.75,4.0,4.25,4.50,4.75,5.0,5.25,5.50,5.75,6.0/
      DATA YF/.720,.280,.003,.046,.037,.012,.006,.040,.570,
          .180,.015,
     *.030,.006,.057,.005,.741,.261,.0026,.774,.234,
     *.711,.287,.0013,5.0E-5,.733,.151,.115,.032,9.0E-6,
          .00021,5.0E-5,
     *8.0E-5,6.0E-6,5.0E-5,3.0E-5,5.0E-6,3.0E-5,8.0E-6,
          7.0E-6,1.5E-5,
     *6.0E-6,2.6E-5,4.0E-6,2.0E-6,.755,.244,.00091,3.0E-5,
          2.1E-7,
     *.0035,.010,.0036,.011,.83,.12,.012,.0003,.74,.26,
          21*1.0/
      DATA TIT/'H    ','N    ','O    ','U-234','U-235',
          'U-236','U-238',
     *'PU238','PU239','PU240','PU241','PU242'/
      IG=51
C     MULTIPLY CROSS SECTIONS BY 1.35 AND CHANGE UNITS FROM
          MB TO BARNS.
      DO 1 I=1,748
1     AN17(I)=AN17(I)*1.35*1.0E-3
      DO 2 I=1,732
2     AN18(I)=AN18(I)*1.35*1.0E-3
      E(1)=1.0
      DO 3 I=2,IG
3     E(I)=E(I-1)+0.1
C     READ IN 13 ATOM DENSITIES H,N,O,U-234,U-235,U-236,
          U-238,PU-238,
C     PU-239,PU-240,PU-241,PU-242,AND THE VOLUME OF THE
C          EXPERIMENT OF INTEREST.
4     READ(5,31) (TITLE(I),I=1,18),IPLOT,ITYPE
      READ(5,*) (N(I),I=1,13)
      IF(N(1).LT.1.0E-10) GO TO 40
C     COMPUTATION OF DENSITIES FOR EACH NUCLIDE OR ELEMENT
      UA=0.0
      PA=0.0
      USUM=0.0
      PSUM=0.0
      DO 5 I=1,12
```

Figure B.1.--Continued

```
      A1(I)=A(I)
      P(I)=(N(I)*A(I)/A(13))*1000.0
      IF((I.GT.3).AND.(I.LT.8)) USUM=USUM+P(I)
      IF((I.GT.3).AND.(I.LT.8)) UA=UA+P(I)*A(I)
      IF(I.GT.7) PSUM=PSUM+P(I)
      IF(I.GT.7) PA=PA+P(I)+A(I)
5     CONTINUE
      A1(13)=A(13)
      AAVG=238.0
      BAVG=239.0
      IF(USUM.NE.0.0) AAVG=UA/USUM
      IF(PSUM.NE.0.0) BAVG=PA/PSUM
C     COMPUTATION OF TOTAL FUEL DENSITY AND ATOM DENSITY OF
           0-17 AND 0-18.
      NO17=N(3)*0.00039
      NO18=N(3)*0.00205
      PF=P(1)+P(2)+P(3)+P(4)+P(5)+P(6)+P(7)
      PF=P(8)+P(9)+P(10)+P(11)+P(12)+PF
      R1=NO17/PF
      R2=NO18/PF
C     COMPUTATION OF EPISLON ALPHA FOR EACH ELEMENT FOR 51
           ENERGY GROUPS
      CALL EPSLON(E,EAH,EAN,EAO,EAU,EAP,IG)
C     COMPUTATION OF (DE/DX) AND (DE/DPX) FOR 51 ENERGY
           GROUPS.
C     IN MEV/CM AND MEV-CM**2/MG.
      CALL SPOWER(EAH,EAN,EAO,EAU,EAP,DEPX,DEX,IG)
      WRITE(6,32) (TITLE(I),I=1,18)
      WRITE(6,33)
      DO 7 I=1,12
      WRITE(6,29) I,E(I),EAH(I),EAN(I),EAO(I),EAU(I),DEX(I),
           DEPX(I),
     *TIT(I),P(I)
7     CONTINUE
      DO 8 I=13,IG
      WRITE(6,30) I,E(I),EAH(I),EAN(I),EAO(I),EAU(I),DEX(I),
           DEPX(I)
8     CONTINUE
      IF(IPLOT.EQ.0) IA=59
      IF(IPLOT.NE.0) IA=80
C     COMPUTATION OF EPISLON ALPHA FOR EACH ELEMENT FOR ALL
C          0-17 AND 0-18 ENERGIES.
      CALL EPSLON(E17,EAH,EAN,EAO,EAU,EAP,748)
      CALL EPSLON(E18,EAH1,EAN1,EAO1,EAU1,EAP1,732)
```

Figure B.1.--Continued

```
C       COMPUTATION OF (DE/DX) AND (DE/DPX) FOR ALL O-17 AND
             O-18 ENERGIES
C       IN MEV/CM AND MEV-CM**2/MG.
        CALL SPOWER(EAH,EAN,EAO,EAU,EAP,DEPX,DEX,748)
        CALL SPOWER(EAH1,EAN1,EAO1,EAU1,EAP1,DEPX1,DEX1,732)
        DO 11 I=1,IA
        XI1=0.0
        XI2-0.0
C       COMPUTATION OF THE INTEGRAL FROM 0.0 TO ALPHAE(I)
             MEV FOR O-17.
C       AND O-18.
        CALL TEGRAL(ALPHAE,DEPX,E17,DE17,AN17,XI1,748,I)
        CALL TEGRAL(ALPHAE,DEPX1,E18,DE18,AN18,XI2,732,I)
C       COMPUTATION OF P(E) FOR O-17 AND O-18.
        P1(I)=R1*XI1
        P2(I)=R2*XI2
11      CONTINUE
C       COMPUTATION OF THE NEUTRON SOURCE FROM THE (ALPHA,N)
             REACTION.
        WRITE(6,32) (TITLE(I),I=1,18)
        WRITE(6,34)
        V=N(13)
        K=0
        SUM1(1)=0.0
        SUM2(1)=0.0
        DO 12 I=1,3
        K=K+1
        S1(K)=V*N(4)*LAMBDA(4)*YF(K)*P1(K)*1.0E+24
        S2(K)=V*N(4)*LAMBDA(4)*YF(K)*P2(K)*1.0E+24
        WRITE(6,25) K,V,ALPHAE(K),YF(K),P1(K),P2(K),N(4),
              LAMBDA(4),
     *S1(K),S2(K)
        SUM1(1)=SUM1(1)+S1(K)
12      SUM2(1)=SUM2(1)+S2(K)
        S(1)=SUM1(1)+SUM2(1)
        WRITE(6,26) SUM1(1),SUM2(1),S(1)
        SUM1(2)=0.0
        SUM2(2)=0.0
        DO 13 I=1,12
```

Figure B.1.--Continued

```
      K=K+1
      S1(K)=V*N(5)*LAMBDA(5)*YF(K)*P1(K)*1.0E+24
      S2(K)=V*N(5)*LAMBDA(5)*YF(K)*P2(K)*1.0E+24
      WRITE(6,25) K,V,ALPHAE(K),YF(K),P1(K),P2(K),N(5),
           LAMBDA(5),
     *S1(K),S2(K)
      SUM1(2)=SUM1(2)+S1(K)
13    SUM2(2)=SUM2(2)+S2(K)
      S(2)=SUM1(2)+SUM2(2)
      WRITE(6,26) SUM1(2),SUM2(2),S(2)
      SUM1(3)=0.0
      SUM2(3)=0.0
      DO 14 I=1,3
      K=K+1
      S1(K)=V*N(6)*LAMBDA(6)*YF(K)*P1(K)*1.0E+24
      S2(K)=V*N(6)*LAMBDA(6)*YF(K)*P2(K)*1.0E+24
      WRITE(6,25) K,V,ALPHAE(K),YF(K),P1(K),P2(K),N(6),
           LAMBDA(6),
     *S1(K),S2(K)
      SUM1(3)=SUM1(3)+S1(K)
14    SUM2(3)=SUM2(3)+S2(K)
      S(3)=SUM1(3)+SUM2(3)
      WRITE(6,26) SUM1(3),SUM2(3),S(3)
      SUM1(4)=0.0
      SUM2(4)=0.0
      DO 15 I=1,2
      K=K+1
      S1(K)=V*N(7)*LAMBDA(7)*YF(K)*P1(K)*1.0E+24
      S2(K)=V*N(7)*LAMBDA(7)*YF(K)*P2(K)*1.0E+24
      WRITE(6,25) K,V,ALPHAE(K),YF(K),P1(K),P2(K),N(7),
           LAMBDA(7),
     *S1(K),S2(K)
      SUM1(4)=SUM1(4)+S1(K)
15    SUM2(4)=SUM2(4)+S2(K)
      S(4)=SUM1(4)+SUM2(4)
      WRITE(6,26) SUM1(4),SUM2(4),S(4)
      SUM1(5)=0.0
      SUM2(5)=0.0
      DO 16 I=1,4
      K=K+1
      S1(K)=V*N(8)*LAMBDA(8)*YF(K)*P1(K)*1.0E+24
      S2(K)=V*N(8)*LAMBDA(8)*YF(K)*P2(K)*1.0E+24
      WRITE(6,25) K,V,ALPHAE(K),YF(K),P1(K),P2(K),N(8),
           LAMBDA(8),
```

Figure B.1.--Continued

```
     *S1(K),S2(K)
      SUM1(5)=SUM1(5)+S1(K)
16    SUM2(5)=SUM2(5)+S2(K)
      S(5)=SUM1(5)+SUM2(5)
      WRITE(6,26) SUM1(5),SUM2(5),S(5)
      SUM1(6)=0.0
      SUM2(6)=0.0
      DO 17 I=1,20
      K=K+1
      S1(K)=V*N(9)*LAMBDA(9)*YF(K)*P1(K)*1.0E+24
      S2(K)=V*N(9)*LAMBDA(9)*YF(K)*P2(K)*1.0E+24
      WRITE(6,25) K,V,ALPHAE(K),YF(K),P1(K),P2(K),N(9),
           LAMBDA(9),
     *S1(K),S2(K)
      SUM1(6)=SUM1(6)+S1(K)
17    SUM2(6)=SUM2(6)+S2(K)
      S(6)=SUM1(6)+SUM2(6)
      WRITE(6,26) SUM1(6),SUM2(6),S(6)
      SUM1(7)=0.0
      SUM2(7)=0.0
      DO 18 I=1,5
      K=K+1
      S1(K)=V*N(10)*LAMBDA(10)*YF(K)*P1(K)*1.0E+24
      S2(K)=V*N(10)*LAMBDA(10)*YF(K)*P2(K)*1.0E+24
      WRITE(6,25) K,V,ALPHAE(K),YF(K),P1(K),P2(K),N(10),
           LAMBDA(10),
     *S1(K),S2(K)
      SUM1(7)=SUM1(7)+S1(K)
18    SUM2(7)=SUM2(7)+S2(K)
      S(7)=SUM1(7)+SUM2(7)
      WRITE(6,26) SUM1(7),SUM2(7),S(7)
      SUM1(8)=0.0
      SUM2(8)=0.0
      DO 19 I=1,8
      K=K+1
      S1(K)=V*N(11)*LAMBDA(11)*YF(K)*P1(K)*1.0E+24
      S2(K)=V*N(11)*LAMBDA(11)*YF(K)*P2(K)*1.0E+24
      WRITE(6,25) K,V,ALPHAE(K),YF(K),P1(K),P2(K),N(11),
           LAMBDA(11),
     *S1(K),S2(K)
      SUM1(8)=SUM1(8)+S1(K)
19    SUM2(8)=SUM2(8)+S2(K)
      S(8)=SUM1(8)+SUM2(8)
      WRITE(6,26) SUM1(8),SUM2(8),S(8)
```

Figure B.1.--Continued

```
      SUM1(9)=0.0
      SUM2(9)=0.0
      DO 20 I=1,2
      K=K+1
      S1(K)=V*N(12)*LAMBDA(12)*YF(K)*P1(K)*1.0E+24
      S2(K)=V*N(12)*LAMBDA(12)*YF(K)*P2(K)*1.0E+24
      WRITE(6,25) K,V,ALPHAE(K),YF(K),P1(K),P2(K),N(12),
          LAMBDA(12),
     *S1(K),S2(K)
      SUM1(9)=SUM1(9)+S1(K)
20    SUM2(9)=SUM2(9)+S2(K)
      S(9)=SUM1(9)+SUM2(9)
      WRITE(6,26) SUM1(9),SUM2(9),S(9)
      SUM=0.0
      DO 21 I=1,9
21    SUM=SUM+S(I)
      WRITE(6,27) SUM
25    FORMAT(I5,1PE15.4,3E12.4,E13.4,E12.4,E13.4,3E12.4)
26    FORMAT(94X,1PE12.4,2E12.4)
27    FORMAT(118X,1PE12.4)
      IF(IPLOT.EQ.0) GO TO 4
      IB=IA-59
      DO 22 I=1,IB
      K=K+1
      WRITE(6,28) K,V,ALPHAE(K),YF(K),P1(K),P2(K)
22    CONTINUE
      GO TO 4
28    FORMAT(I5,1PE15.4,3E12.4,E13.4)
29    FORMAT(I5,1PE15.4,E14.4,E15.4,E14.4,3E15.4,5X,A5,1X,
          E11.4)
30    FORMAT(I5,1PE15.4,E14.4,E15.4,E14.4,3E15.4)
31    FORMAT(18A4,2I4)
32    FORMAT(1H1,18A4,//)
33    FORMAT('                              ALPHA PARTICLE STOPPING
          CROSS SECTIO
     1NS AS A FUNCTION OF   STOPPING POWER AS A FUNCTION',/,'
          ENERGY
     2 ALPHA      ENERGY FOR HYDROGEN, NITROGEN, OXYGEN, AND
          URANIUM
     3              OF ENERGY            NUCLIDE   NUCLIDE',/'
     4' GROUPS    ENERGY              (ELECTRON VOLTS/(1.0E+15
          ATOMS/CM*
     5*2))                  DE/DX         DE/DPX        OR
                 DENSITY',
```

Figure B.1.--Continued

```
     6/,'             (MEV)         HYDROGEN        NITROGEN
                OXYGEN
     7       URANIUM          (MEV/CM)     (MEV-CM**2/MG)
              ELEMENT (MG/CM**3
     8)',/)
34    FORMAT(12X,'VOLUME       ALPHA',43X,'URANIUM
           URANIUM          0-
     117         0-18         TOTAL',/,'  ALPHA     OF CRAC
                 PARTICLE
     2              0-17          0-18      ISOTOPE ATOM ISOTOPE
          DECAY  NEU
     3TRON       NEUTRON      NEUTRON',/,' PARTICLE EXPERIMENT
                 ENERGY
     4 BRANCHING    (ALPHA,N)     (ALPHA,N)     DENSITIES
                 CONSTANTS     S
     5OURCE        SOURCE       SOURCE',/,'  NUMBER    (CM**3)
                   (MEV)
     6    FRACTION  PROBABILITY  PROBABILITY (ATOMS/B-CM)
                   (SEC-1)
     7(N/SEC)       (N/SEC)      (N/SEC)',/)
35    FORMAT(4(2F7.4,F6.2))
40    STOP
      END

      SUBROUTINE EPSLON(E,EAH,EAN,EAO,EAU,EAP,K)
      IMPLICIT REAL*8 (A-H,L-Z)
      DIMENSION E(K),EAH(K),EAN(K),EAO(K),EAU(K),EAP(K)
      DO 1 I=1,K
      E(I)=E(I)*1000.0
      SLH=0.9661*E(I)**0.4126
      SLN=2.51*E(I)**0.4752
      SLO=1.766*E(I)**0.5261
      SLU=5.218*E(I)**0.5828
      SLP=5.218*E(I)**0.5828
      SHH=(6920.0/E(I))*DLOG(1.0+(8831.0/E(I))+0.002582*E(I))
      SHN=(38260.0/E(I))*DLOG(1.0+(13020.0/E(I))+0.001892*
          E(I))
      SHO=(37110.0/E(I))*DLOG(1.0+(15240.0/E(I))+0.002804*
          E(I))
      SHU=(245000.0/E(I))*DLOG(1.0+(3838.0/E(I))+0.00125*E(I))
      SHP=(245000.0/E(I))*DLOG(1.0+(3838.0/E(I))+0.00125*E(I))
      EAH(I)=SLH*SHH/(SLH+SHH)
      EAN(I)=SLN*SHN/(SLN+SHN)
```

Figure B.1.--Continued

```
      EAO(I)=SLO*SHO/(SLO+SHO)
      EAU(I)=SLU*SHU/(SLU+SHU)
      EAP(I)=SLP*SHP/(SLP+SHP)
1     E(I)=E(I)*0.001
      RETURN
      END

      SUBROUTINE SPOWER(EAH,EAN,EAO,EAU,EAP,DEPX,DEX,K)
      IMPLICIT REAL*8 (A-H,L-Z)
      COMMON /MSP/ N(13),P(13),A(13),PF,AAVG,BAVG,ITYPE
      DIMENSION EAH(K),EAN(K),EAO(K),EAU(K),EAP(K),DEPX(K),
           DEX(K)

      DO 1 J=1,K
      DEPX(J)=(A(13)/PF)*((P(1)*EAH(J)/A(1))+(P(2)*EAN(J)/
           A(2))+
     *(P(3)*EAO(J)/A(3))+((P(4)+P(5)+P(6)+P(7))*EAU(J)/AAVG)+
     *((P(8)+P(9)+P(10)+P(11)+P(12))*EAP(J)/BAVG))
      IF(ITYPE.EQ.1) DEPX(J)=(A(13)/PF)*(
     *(P(3)*EAO(J)/A(3))+((P(4)+P(5)+P(6)+P(7))*EAU(J)/AAVG)+
     *((P(8)+P(9)+P(10)+P(11)+P(12))*EAP(J)/BAVG))
      DEX(J)=(EAH(J)*N(1)+EAN(J)*N(2)+EAO(J)*N(3)+EAU(J)*
           (N(4)+N(5)+
     *N(6)+N(7))+EAP(J)*(N(8)+N(9)+N(10)+N(11)+N(12)))*1000.0
1     CONTINUE
      RETURN
      END

      SUBROUTINE TEGRAL(ALPHAE,DEPX,E,DE,AN,XI,K,I)
      IMPLICIT REAL*8 (A-H,L-Z)
      DIMENSION ALPHAE(80),DEPX(K),E(K),DE(K),AN(K)
      DO 1 J=1,K
      IF(E(J).GT.ALPHAE(I)) GO TO 2
1     XI=XI+AN(J)*DE(J)/DEPX(J)
2     RETURN
      END
```

Figure B.1.--Continued

```
      C****PROGRAM CRAC (INPUT,OUTPUT,TAPE5=INPUT,TAPE6=
     1        OUTPUT)
            IMPLICIT REAL*8 (A-H,K,N-Z)
            DIMENSION DELTA(29)
      C
      C****   SET THE CONSTANTS
      C
            DATA DELTA/.48,.46,.48,.26,.24,.07,.08,.16,.27,
           2.42,.18,.25,.08,.08,.26,.09,.14,.06,.09,.14,.16,
           3.26,.46,.48,.32,.14,.36,.06,.06/
      C
      C****   PRINT THE HEADINGS
      C
       200 FORMAT(1H1,//,45X,"PROBABILITY DATA FOR THE ",
           1  "300MM DIA CYLINDER",//,2X,"EXPERIMENT",
           2 10X,"S",23X,"T",23X,"A",22X,"T1",20X,"P(T1)",/,
           3 4X,"NUMBER",7X,"NEUTRONS/SEC",16X,"SEC",
           4 19X,"SEC**-1",18X,"SEC",19X,"SEC**-1",//)
      C
      C****   DO THE ITERATION AS MANY TIMES AS NECESSARY
      C
            DO 1 I=1,29
            READ(5,100) NAME,S,T,A,TLOW
       100 FORMAT(A8,2X,4F10.5)
            IF(I.LT.23) WRITE(6,200)
            IF(I.GE.23) WRITE(6,201)
       201 FORMAT(//,45X,"PROBABILITY DATA FOR THE 800MM ",
           1  "DIA CYLINDER",//,2X,"EXPERIMENT",
           2 10X,"S",23X,"T",23X,"A",22X,"T1",20X,"P(T1)",/,
           3 4X,"NUMBER",7X,"NEUTRONS/SEC",16X,"SEC"
           4 19X,"SEC**-1",18X,"SEC",19X,"SEC**-1",//)
      C
      C****   NOW THE CALCULATIONS
      C
       3    DO 2 J=1,50
            B=FLOAT(J)
            T1=(TLOW-DELTA(I)) + B*DELTA(I)
            DUM1=2.0D0*A*S/1.952D0
            DUM2=A*S/1.952D0
            DUM3=DUM2*T1**2.0D0
            DUM4=DEXP(-DUM3)
            PT1=DUM1*T1*DUM4
      C
      C****   OUTPUT THE RESULTS
      C
```

Figure B.2. List of CRAC.

```
45          WRITE(6,203)NAME,S,T,A,T1,PT1
          203 FORMAT(4X,A8,4X,5(1PD16.9.7X))
          2   CONTINUE
          1   CONTINUE
              STOP
              END
```

Figure B.2.--Continued

```
      C****PROGRAM AGNS (INPUT,OUTPUT,TAPE5=INPUT,TAPE6=
     1        OUTPUT)
           IMPLICIT REAL*8 (A-H,K,N-Z)
      C
      C****   SET THE CONSTANTS
      C
           DELTA=0.2195
           EPS=1.0D-28
      C
      C****   PRINT THE HEADINGS
      C
           WRITE(6,200)
       200 FORMAT(1H1,//,39X,"PROBABILITY DATA FOR THE ",
          1  "800MM DIA DISSOLVER TANK",//,2X,"EXPERIMENT",
          2 10X,"S",23X,"T",23X,"A",22X,"T1",20X,"P(T1)",/,
          3 4X,"NUMBER",7X,"NEUTRONS/SEC",16X,"SEC",
          4 19X,"SEC**-1",18X,"SEC",19X,"SEC**-1",//)
      C
      C    *  *  *  *  *  *  *  *  *  *  *  *  *  *  *  *  *
      C
           READ(5,100) NAME,S,T,A,TLOW
       100 FORMAT(A7,3X,4F10.5)
      C
      C****   NOW THE CALCULATIONS
      C
       3   DO 2 J=1,2000
           B=FLOAT(J)
           T1=(TLOW-DELTA) + B*DELTA
           K=2.0D0*S*T/1.840D0
           N=DSQRT(A/(2.0D0*T))*T1
           DUM1=DSQRT((2.0D0*A*T*S**2.0D0)/10.636D0)
           DUM2=DEXP(-N*N)
           DUM3=1.0D0-K
           CALL ERF(N,EPS,DUMMY2,IERR)
           IF(IERR .GT. 0) GO TO 5
           DUMMY=1.0D0-DUMMY2
           PT1=DUM1*(DUM2/(5.0D-01*DUMMY)**DUM3)
      C
      C****   OUTPUT THE RESULTS
      C
           WRITE(6,203)NAME,S,T,A,T1,PT1
       203 FORMAT(4X,A7,4X,5(1PD16.9,7X))
           IF(PT1 .LT. 1.0D-06) GO TO 5
```

Figure B.3. List of AGNS.

```
      2   CONTINUE
      5   WRITE(6,202)
45    202 FORMAT(//)
          STOP
          END


 1        SUBROUTINE ERF(N,EPS,Y,IERR)
          IMPLICIT DOUBLE PRECISION(A-H,N-Z)
          IF(N .EQ. 0) GO TO 3
          IERR=0
 5        IF(DABS(N) .GT. 7.5D0) IERR=1
          SUM=0.0D0
          F=1.0D0
          IF(N .LT. 0) F=-1.0D0
          N=DABS(N)
10        A=2.0D0/3.0D0
          PI=3.14159265358979323846264338327 9D0
          DO 1 M=1,1000
          FM=FLOAT(M)
          TERM=A*N**(2.0D0*M+1.0D0)
15        A=A*2.0D0/(2.0D0*FM+3.0D0)
          SUM=SUM+TERM
          ERROR=TERM/SUM
          IF(ERROR .LE. EPS) GO TO 2
        1 CONTINUE
20      2 CONTINUE
          SUM=SUM+N
          Y=SUM*(2,0D0/DSQRT(PI))*DEXP(-N*N)
          Y=Y*F
          RETURN
25      3 CONTINUE
          Y=0.0D0
          EPS=0.0D0
          RETURN
          END
```

Figure B.3.--Continued

REFERENCES

Bair, J. K. and Gomez del Campo, J., "Neutron Yields from Alpha-Particle Bombardment," Nuclear Science and Engineering, Vol. 71, 18-28, July 1979.

Bair, J. K. and Haas, F. X., "Total Neutron Yield from the Reactions $^{13}C(\alpha,n)O^{16}$ and $^{17,18}O(\alpha,n)Ne^{20,21}$," Phys. Rev. C, Vol. 7, No. 4, 1356-1364, April 1973.

Bair, J. K. and Willard, H. B., "Level Structure in Ne^{22} and Si^{30} from the Reactions $^{18}O(\alpha,n)Ne^{21}$ and $^{26}Mg(\alpha,n)Si^{29}$," Phys. Rev., Vol. 128, No. 1, 299-304, October 1962.

Barbry, F. Y., Memo to R. L. Seale, Sept. 8, 1976.

Browne, E., Dairiki, J. M., Doebler, R. E., Table of Isotopes, Seventh Edition, Copyright 1978.

Carter, R. D., Kiel, G. R., Ridgway, K. R., ARH-600 Criticality Handbook, Vol. II, pgs. III.B.10(5) -1 & -2 and III.B.10 (93.5) -1 & -2, May 1969.

Dyer, H. R., Union Carbide Corporation, K-25 Plant, personal communication, September 1981.

Forehand, H. M., Memo from Los Alamos Scientific Laboratory, Los Alamos, NM, October 1981.

Hansen, G. E., "Assembly of Fissionable Material in the Presence of a Weak Neutron Source," Nuclear Science and Engineering, Vol. 8, 709-719, August 1960.

Johnson, D. L. and Ombrellaro, P. A., "Calculation of Neutron Source Strength in Fast Flux Test Facility Fuel as a Function of Irradiation," Nuclear Technology, Vol. 54, 180-200, August 1981.

Lamarsh, J. R., Introduction to Nuclear Reactor Theory, pgs. 20-22, Addison-Wesley Publishing Company, Reading, Massachusetts, September 1972.

Lécorché, P. and Seale, R. L., "A Review of the Experiments Performed to Determine the Radiological Consequences of a Criticality Accident," USAEC Report Y-CDC-12, Union Carbide Corporation, Y-12 Plant, Nov. 3, 1973.

McLaughlin, T. P., "Investigation of the 10/17/78 Criticality Incident in the Uranium Extraction Process Scrub Column at the ICPP," Idaho National Engineering Laboratory, U.S. Dept. of Energy Idaho Operations Office, Nov. 1978.

Paxton, H. C., "Criticality Control in Operations with Fissile Material," USAEC Report LA-3366 (Rev.), Los Alamos Scientific Laboratory, Los Alamos, NM, Nov. 1972.

Stratton, W. R., "A Review of Criticality Accidents," USAEC Report LA-3611, Los Alamos Scientific Laboratory, Los Alamos, NM, 1967.

Terrell, J., "Distributions of Fission Neutron Numbers," Phys. Rev., Vol. 108, No. 3, 783-789, November 1957.

Verdon, C. P., "Report on the AGNS Dissolver Tank," University of Arizona, 1975.

Ziegler, J. F., "Helium: Stopping Powers and Ranges in all Elemental Metter," Stopping and Ranges of Ions in Matter, Vol. 4, Pergamon Press, New York, 1977.

Ziegler, J. F. and Chu, W. K., "Stopping Cross Sections and Backscattering Factors for ^{4}He Ions in Matter," Atomic Data and Nuclear Data Tables, Vol. 13, No. 5, 463-489, May 1974.